Realia et Realia naturalia

ANDRIS SLAVINSKIS

ESTCube-1 attitude determination

TARTU ÜLIKOOL · UNIVERSITAS TARTUENSIS
1632

ANDRIS SLAVINSKIS

ESTCube-1 attitude determination

This study was carried out at Tartu Observatory, the University of Tartu, the Finnish Meteorological Institute and in the Estonian Student Satellite Programme.

The dissertation was submitted on October 23rd, 2015, in partial fulfilment of the requirements for the degree of Doctor of Philosophy in physics (space technology), and allowed for defence by the Council of the Institute of Physics, University of Tartu.

Supervisor: Dr. Mart Noorma,
               Tartu Observatory,
               University of Tartu,
               Estonia

Opponent: Dr. Linas Bukauskas,
               University of Vilnius,
               Lithuania

Defence: November 26th, 2015, University of Tartu, Estonia

University of Tartu Press
www.tyk.ee

Contents

List of original publications

This thesis is based on the following publications:

[I] Lätt, S., **Slavinskis, A.**, Ilbis, E., Kvell, U., Voormansik, K., Kulu, E. et al. (2014). "ESTCube-1 nanosatellite for electric solar wind sail in-orbit technology demonstration." *Proc. Estonian Acad. Sci.*, 63(2S), 200–209.

[II] **Slavinskis, A.**, Kvell, U., Kulu, E., Sünter, I., Kuuste, H., Lätt, S. et al. (2014). "High spin rate magnetic controller for nanosatellites." *Acta Astronaut.*, 95, 218–226.

[III] **Slavinskis, A.**, Kulu, E., Viru, J., Valner, R., Ehrpais, H., Uiboupin, T. et al. (2014). "Attitude determination and control for centrifugal tether deployment on ESTCube-1 nanosatellite." *Proc. Estonian Acad. Sci.*, 63(2S), 242–249.

[IV] **Slavinskis, A.**, Ehrpais, H., Kuuste, H., Sünter, I., Viru, J., Kulu, E. et al. (2015). "Flight results of ESTCube-1 attitude determination system." *Journal of Aerospace Engineering*, DOI: 10.1061/(ASCE)AS.1943-5525.0000504, 04015014.

Other related publications:

1. **Slavinskis, A.**, Kuuste, H., Ilbis, E., Pajusalu, M., Eenmäe, T, Sünter, I. et al. (2015). "ESTCube-1 in-orbit experience and lessons learned." *IEEE Aerosp. Electron. Syst. Mag.* 30(8), 12–22.

Author's contribution

The articles on which this thesis is based are the result of collective work and contain important contributions from all the co-authors. During the time when all publications of this thesis were prepared and written, the author was leading the ESTCube-1 attitude determination and control system. He has co-supervised four bachelor theses that give major contributions to publications [II], [III] and [IV]. The author's contribution to the publications referred to by their Roman numerals is indicated as follows:

[I] Deriving the formula for spin rate change; communicating with and gathering information from the co-authors; preparing Figure 2 and revising all other figures; writing of the following sections and subsections: Introduction, Mission analysis, Satellite design, Attitude determination and control, Payload, Camera and Conclusions; harmonising the whole text.

[II] Porting the Kalman filter and the spin-up controller from MATLAB to C; preparing and running simulations; analysing results; preparing all figures and the table; writing the whole text.

[III] Gathering laboratory results from co-authors; preparing and running simulations; analysing results; preparing Figures 1, 5, 6, and 7; revising all figures; writing the whole text.

[IV] An updated version of the Kalman filter (Publication [II]) was used on board; preparing uncertainty budgets; performing initial data analysis; supervising data analysis; preparing all figures and tables; writing the whole text.

Abbreviations

ADC	Analogue to Digital Converter
ADS	Attitude Determination System
CDHS	Command and Data Handling System
COTS	Commercial Off-The-Shelf
FoV	Field of View
IGRF	International Geomagnetic Reference Field
IOD	In-Orbit Demonstration
LEO	Low Earth Orbit
NORAD	North American Aerospace Defense Command
TLE	Two-Line Element set
TRL	Technology Readiness Level
PSD	Position Sensitive Devices
UKF	Unscented Kalman Filter

Chapter 1
Introduction

The focus of our work is to develop testing platforms for In-Orbit Demonstration (IOD) of novel propulsion technologies. This thesis presents an Attitude Determination System (ADS) developed for testing electric solar wind sail (E-sail) technology on board the ESTCube-1 satellite. The system uses Sun sensors, magnetometers, gyroscopic sensors for attitude measurements and a Kalman filter for attitude estimation. The ADS has been calibrated and characterised in the laboratory, simulated, as well as recalibrated and characterised in orbit.

1.1 Background

Spacecraft propulsion is an enabler of space exploration. It enables launching objects from the Earth's surface, for changing orbits, for escaping the Earth's orbit, for approaching other celestial bodies and even landing on them. While conventional propulsion methods like chemical, ion and cold gas have served the drive of exploration for decades, the first space exploration visionaries and science fiction writers also described and discussed propellantless means of propulsion [1–4]. One of the most popular technologies is the photon sail, which employs a large reflective sail to capture thrust from photons coming from the Sun [5–7]. In recant decades, other types of sails have been proposed, for example, the magnetic sail and the E-sail. The magnetic sail consists of a magnetic field generated around a spacecraft and deflecting the solar wind [8; 9]. The E-sail consists of centrifugally stretched and positively charged tethers that also deflect charged particles in the solar wind [10; 11]. The E-sail is a promising propulsion system concept because it provides a high and constant thrust with its large effective sail area and small mass [12]. The E-sail has the potential to decrease the cost of interplanetary travel and, at the same time, it allows for faster travel speeds and enables new missions [13–19]. A satellite with one or more negatively charged E-sail tethers can be used in Low Earth Orbit (LEO) to deorbit satellites [20; 21].

The E-sail has been developed to Technology Readiness Level (TRL) 4–5 [22; 23]. In order to increase the TRL further, technology has to be demonstrated in orbit. For IOD, the stepping stone approach can be employed, first, by testing the technology in LEO. Here instead of the solar wind plasma stream there is ionospheric plasma, which moves relative to the satellite due

to the orbital motion of the satellite. Second, the technology is tested in an authentic environment — the solar wind. By demonstrating technology in LEO, the E-sail TRL would increase to 6 and the plasma brake TRL to 7 or even 9 if a satellite is effectively deorbited. By demonstrating technology in the solar wind, the E-sail TRL would increase to 7. TRL 9 can be reached by using the E-sail in an operational mission.

According to the E-sail inventor Pekka Janhunen [12], the tether is produced by an ultrasonic wire-to-wire bonding method [24]. A tether of one kilometre has been successfully produced [25]. The reeling system has been developed based on a piezoelectric motor [26; 27]. The reeling system assists tether deployment — the pull and tension is provided by the centrifugal force and an end-mass at the tip of the tether [**III**]. To provide centrifugal force, high rate spin control is required [**II**].

Since the end of 1990s, nanosatellites (1–10 kg) have grown from simple, mostly educational, satellites with limited functionality to platforms for IOD, Earth observation, scientific experiments and even operational missions [28–35]. One of the biggest challenges in such missions is to provide accurate on-board attitude determination that is usually required by a payload and/or for attitude control. The small size of nanosatellites introduces limiting factors on performance and on means of accurate on-board attitude determination. Due to the small size and affordability, the most popular sensors for nanosatellite ADSs are magnetometers, Sun sensors and gyroscopic sensors, e.g., [36–43]. Star trackers are also becoming more and more popular since ADSs with higher accuracy are required and star trackers suitable for nanosatellites have been developed [36; 44–46]. Rapid developments in consumer electronics have provided Commercial Off-The-Shelf (COTS) components, which are miniaturised and can provide high processing power. Such components are successfully used on nanosatellites but require thorough testing.

In order to demonstrate affordable in-orbit tether deployment and to measure the E-sail force, a cost-effective approach with quick development time has to be used. Hence nanosatellites are employed to perform proof of concept tests. The first E-sail IOD was carried out on board the ESTCube-1 satellite which was launched in May 2013 [**I**]. In-orbit tests were carried out in the autumn of 2014 and provided suggestions for further development of the tether deployment system [47]. The second IOD with an improved tether deployment system will be tested on board the Aalto-1 satellite which will be launched at the beginning of 2016 [36; 48].

While nowadays high performance nanosatellite ADSs and other subsystems are available commercially, in 2008, when the ESTCube-1 project

started, on-board attitude determination was only being demonstrated on some nanosatellites. Such satellites were mostly equipped with passive attitude control systems (i.e., with permanent magnets following the Earth's magnetic field or with booms employing gravity gradient stabilisation) and attitude determination was rarely performed on board [28]. To the best knowledge of the author, an active on-board ADS for high rate spin control has not been developed previously.

1.2 Progress in this work

This work presents development and characterisation of an ADS for the first E-sail experiment on board ESTCube-1. The satellite was launched on May 7, 2013 and this work also presents in-orbit validation of the ADS. ESTCube-1 is required to spin up to one rotation per second for centrifugal tether deployment [I]. Feasibility of high rate spin up has been demonstrated by simulations, which also set the preliminary requirements for attitude determination accuracy [II]. ESTCube-1 is required to determine the attitude with an accuracy better than 2°. The ADS was developed and characterised in the laboratory. Results of laboratory characterisation were used to demonstrate the feasibility of determining the attitude with the required accuracy using simulations [III]. With in-orbit recalibration and validation, the ADS was significantly improved. The system was characterised by developing an uncertainty budget, which showed that the ADS fulfils the requirements for attitude determination accuracy. The attitude determined from on-board camera images was used as a reference. The uncertainty budget includes uncertainties from both attitude determination methods [IV].

Chapter 2
Mission objectives and attitude determination requirements

The ESTCube-1 scientific mission objective was to perform an IOD of the E-sail. While the E-sail operational environment is the solar wind, a proof of concept can be demonstrated in the Earth's surrounding ionosphere, which moves relative to the satellite due to the orbital motion of the satellite. The ionospheric plasma stream is up to 10^5 denser than the solar wind but the relative speed is 50 to 100 times slower. The expected E-sail thrust per unit length in ESTCube-1 was ~ 1 μN [12].

To provide a cost-efficient solution for demonstrating the E-sail, ESTCube-1 was built according to the CubeSat standard. CubeSats are satellites whose size is either $\approx 10 \times 10 \times 10$ cm and mass is ≈ 1 kg corresponding to one unit, or a combination of multiple units [49]. By the time when the ESTCube-1 project started, more than 40 CubeSats had been launched, by the time of the ESTCube-1 launch, more than 110 CubeSats had been launched and, up to now, more than 380 CubeSats have been launched [50]. Popularity of the standard, especially between university satellite projects, has created a market of various launch options. This has been enabled by a standardised satellite deployer and cost-effectiveness as a result of the use and testing of consumer electronics and availability of COTS subsystems. The initial study showed the feasibility of fulfilling the ESTCube-1 scientific mission objective by using a one-unit CubeSat form factor, which sets the volume of satellite components and subsystems as the main design driver.

The socioeconomic objectives of the project are to provide hands-on education to students and pupils, as well as to popularise science and space exploration. ESTCube-1 was built within the Estonian Student Satellite Programme where students and pupils were developing the satellite and managing the project under supervision of advisors. The ESTCube-1 project was coordinated by the University of Tartu and Tartu Observatory where most of the satellite bus development and integration took place. Students from Tallinn University of Technology, the Estonian Aviation Academy, the Estonian University of Life Sciences, Ventspils University College, University of Latvia and Bremen University of Applied Sciences also contributed to the project. The payload was developed by the Finnish Meteorological Institute, University of Helsinki, University of Jyväskylä, University Of Eastern Finland and the

German Aerospace Center.

The satellite payload consists of a tether, a motor with a reel for storing the tether, an end-mass at the tip of the tether, a high voltage source for charging the tether, a slip ring and electron guns [26].

Requirements for the ADS were directly related to system requirements, which stem from the main mission objective to test components of E-sail technology. The experiment consists of the following steps [**I**].

1. Spin up the satellite to one rotation per second and align the spin axis with the Earth's polar axis. An on-board ADS is required to provide inputs to the spin controller.

2. Deploy the E-sail tether using the centrifugal force such that the tether is in the spin plane. The ADS is required to monitor changes in the spin rate caused by the changing moment of inertia. It also triggers the camera to take images of the tether end-mass on a dark background.

3. Measure angular velocity changes caused by the Coulomb drag interaction between the charged tether and the surrounding ionospheric plasma. Here the attitude measurements are the main means of determining the E-sail force. The ADS also triggers the charging of the tether in synchronisation with the satellite spin — either up or down the plasma stream depending on the experiment mode.

An equatorial orbit is the most suitable for the E-sail experiment because the experiment can be performed anywhere in this orbit, but ESTCube-1 was designed for a polar orbit because of more frequent launch opportunities, more ground station options and the ability to perform three-axis attitude control with magnetorquers [12]. In a polar orbit, the experiment can be performed over geographical poles where the spin plane is roughly aligned with the plasma stream and the spin axis is nearly parallel to the magnetic field of the Earth (Figure 2.1). In such conditions, the magnetic Lorentz force and the E-sail force are roughly parallel to the spin plane, hence the spin axis will not have a tendency to turn. With $\pm 15°$ from the Earth's poles being the part of orbit where the E-sail experiment can be performed, it was estimated that the E-sail thrust would change the angular rate ≈ 0.5 deg·s^{-1} during one polar pass [**I**].
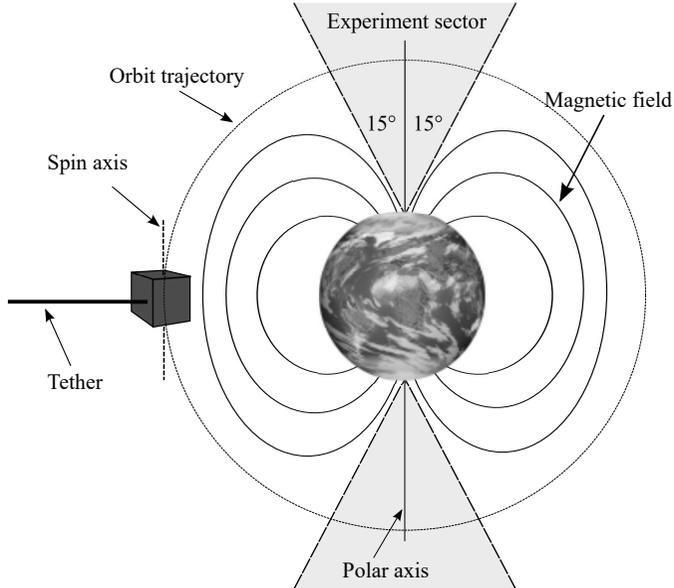
Figure 2.1: Spin plane orientation with respect to the polar orbit. Grey sectors mark where the E-sail experiment is performed. [51]

The high rate spin-up manoeuvre was considered (and later proved to be) the most challenging task for the ESTCube-1 attitude determination and control system. In order to set requirements for the ADS, a simulation study of high rate spin-up for nanosatellites was carried out [II]. The study showed the feasibility to spin up a CubeSat to one rotation per second and align the spin axis with the Earth's polar axis with a pointing error less than $3°$ within three orbits when the satellite was fully operational. By simulating the ADS with limited functionality (large attitude determination error introduced by non-operational Sun sensors), it was found that ten orbits are required to spin up the satellite. From standard deviations used for a fully operational satellite, the preliminary requirement for the attitude determination system was set: standard deviation for magnetic field vector direction of less than $3°$, for Sun direction — $3.33°$ and for angular velocity — 1 deg·s^{-1}. The parameters were not strictly defined at that stage because the uncertainties are the subjects of trade between sensors because sensor measurements are fused during the attitude estimation process. Moreover, detailed mission analysis suggested an attitude determination uncertainty of $\pm 2°$ (95% confidence level, $k = 2$) [III].

Chapter 3
Attitude determination system

The attitude of a spacecraft is its orientation in space. The attitude and its motion describe a rotation of a spacecraft body about the centre of mass. While the orbital position and velocity are independent of the attitude, in many cases it is required in the attitude determination process. Attitude determination is the process of computing the orientation of the spacecraft relative to a reference frame. Inputs to attitude determination computations are measurements of sensors and reference models. Although attitude prediction is defined separately as the process of forecasting the future orientation of the spacecraft, in this thesis, attitude determination will include both processes mostly because the Kalman filter, used for ESTCube-1 attitude estimation, includes a prediction step. [52]

3.1 Reference frames

For attitude determination, reference frames are used to define, for example, the attitude and orientation of one frame with respect to another, to define position and orientation of attitude sensors, and to define principal axes of a satellite. Reference frames are defined by the location of the origin and the direction of axes. A simulation environment developed at Aalborg University for the AAUSAT3 mission [53] was used to simulate the ESTCube-1 ADS. Reference frames implemented in the simulation environment are suitable for the ESTCube-1 mission.

3.1.1 Earth Centred Inertial reference frame (ECI)

As the name of the ECI suggests, its origin is located at the centre of the Earth. The x-axis goes through the point where the vernal equinox and the equatorial plane cross, the z-axis through the Geographic North Pole, and the y-axis is the cross product between the x- and the z-axis. One has to keep in mind that this frame is not perfectly inertial because of the Earth's orbital motion around the Sun, precession of equinoxes and nutation of the Earth's spin axis [52; 54]. The latter two of these factors are included in the uncertainty budget [**IV, Table 1**], but the former one does not influence ESTCube-1 attitude measurements because stars are not used as a reference,

and for attitude determination in general, it can be neglected because of its small influence (≪1 arcsecond) [55].

3.1.2 Earth Centred Earth Fixed reference frame (ECEF)

The ECEF frame is fixed with respect to the surface of the Earth. The origin is in the centre of the Earth with the x-axis crossing the point where the Greenwich meridian crosses the equatorial plane, the z-axis crossing the Geographical North Pole, and the y-axis is the cross product between the x- and the z-axis.

3.1.3 Satellite Body Reference Frame (SBRF)

The SBRF axes are aligned with the satellite frame as shown in Figure 3.1. The tether is deployed in the $+y$ direction and the camera is placed in the same direction to take images of the tether end-mass. The intended spin axis is the z-axis to provide centrifugal force for tether deployment. Electron guns are placed on the $-z$ side. Sun sensors are placed on all sides of the satellite. An exploded view with much more detail of the satellite is presented in [**I, Figure 4**].

Figure 3.1: ESTCube-1 satellite with axes. Photo: Mihkel Pajusalu.

3.1.4 Principal Axes Reference Frame (PARF)

The PARF is a body-fixed frame in which the moment of inertia matrix is diagonal [56]. Its origin is located at the centre of mass with the x-axis being the minor axis of inertia, and the z-axis being the major axis of inertia. The y-axis is the intermediate axis of inertia and also the cross product between the x- and the z-axis. In order to find the centre of mass and principal axes, mass distribution and an inertia matrix must be determined [57]. Hence precision of the PARF depends on measurement or model accuracy.

3.2 Sensors

Attitude determination sensors are used to measure the direction or position of celestial bodies, the Earth or their magnetic field, as well as to take inertial measurements, like the spin rate. The most popular attitude sensors are Sun sensors, magnetometers, Earth sensors, star trackers and angular velocity sensors. Measurements of the direction and position are combined with respective reference models to determine the attitude of the satellite. Inertial measurements are used as an input for dynamic models, hence provide better attitude estimates.

3.2.1 Sun sensors

Sun sensors are widely used for attitude determination for multiple reasons. First, the Sun vector is easy to measure because of the small angular radius of the Sun (0.267° at the distance of one astronomical unit, [52]). The small angular radius of the Sun for most of the cases can be considered as a point light source and hence allows for simpler sensors and algorithms. Second, most of the space missions require sunlight for power and many of them require the pointing of solar panels towards the Sun. Third, the direction of the Sun drives the thermal design. Four, there are missions that require instruments to be pointed towards the Sun. Five, there are instruments that can malfunction when pointed towards the Sun.

Sun sensors can be divided into three groups. Analogue sensors output a continuous signal as a function of the angle of incidence. Course sensors also use analogue detectors but can only detect whether or not the Sun is in the Field of View (FoV). Digital sensors output a discrete signal of a function of the angle of incidence.

Analogue Sun sensors

Analogue Sun sensors are based on Position Sensitive Devices (PSDs) that output current proportional to the cosine of the angle between the sensor normal vector and the incident solar radiation vector [56]. The exact model of a sensor depends on its specific implementation and in most of the cases correction a function has to be determined based on calibration results. The model might need to take into account slit width of the sensor mask, internal reflections in the sensor, thickness of the mask, light coming from other sources like the Earth's albedo, and other effects. When characterising Sun sensors and other sensors, attention should be paid to systematic and random error. Random error is caused by unknown or unpredictable effects, like measurement noise. Although it is not possible to compensate for random error, it can usually be reduced by increasing the number of measurements and filtering them. Systematic errors include bias, gain error, nonlinearity, asymmetry (different gains for positive and negative measurements), quantisation and other known and predictable effects. These errors can be caused by changing temperature, uncertain reference, imperfect sensor design or test bench. Systematic error can be quantified and compensated for. [58; 59]

Digital Sun sensors

Digital Sun sensors nowadays are similar to analogue ones, but instead of PSDs, complementary metal-oxide-semiconductors or charge-coupled devices are used as detectors. They can achieve higher accuracies but the complexity and power consumption are increased, and the sampling rate and the minimum required exposure time limit their use at high spin rates.

Course Sun sensors

Photodiodes, photocells or solar cells are used as course Sun sensors to detect whether the Sun is in the FoV. Due to simplicity, robustness and independence from other attitude measurements, course Sun sensors are suitable for safeguarding instruments, elementary thermal control, safe modes and preliminary attitude acquisition [58].

3.2.2 Magnetometers

A magnetometer measures the magnitude and the direction of the local magnetic field. By using three one-axis magnetometers or one three-axis magnetometer, the magnetic field in all directions can be measured. By combining the measurement with the orientation of the sensor in the SBRF, the magnetic

field in the SBRF can be determined. To interpret the magnetic field vector in, for example, an Earth reference frame, an Earth magnetic field reference model has to be employed [52].

While most types of magnetometers are low-accuracy sensors (order of magnitude of 1°) for attitude determination purposes, their main advantage is that the FoV is not a limit. However, magnetometer measurements can be influenced by the magnetic field of the satellite. The residual magnetic field can be caused by ferromagnetic materials used in satellite structure or current loops in satellite electronics. To avoid the influence of the magnetic field of the satellite, magnetometers have to be calibrated and they are sometimes placed outside the main structure of the satellite — on a boom. Magnetometers are also limited as attitude determination sensors since they can only be used inside the Earth's magnetosphere (mostly below 1000 km where the magnetic field is strong enough [52]).

When magnetometers are used in combination with magnetic torquers, it should be checked that the magnetic field generated by torquers does not influence magnetometer measurements [47]. The easiest way to avoid this is by taking measurements and running torquers in a sequence [**IV, Figure 2**].

On satellites, usually the following types of magnetometers are used: fluxgate, search-coil, Overhauser, and anisotropic magnetoresistive. The first two types have been used on large satellites for decades, the third type is used on geomagnetic missions due to its accuracy in magnetic field magnitude measurements (± 1 nT for 98% of the data [60]) but it has high power consumption. The fourth type is available as miniaturised COTS sensors, hence is popular on nanosatellites. [52; 61]

3.2.3 Earth sensors

Earth sensors are particularly useful for nadir pointing satellites, for example, Earth observation, communication and weather. Earth sensors detect the Earth horizon and from that it is possible to determine attitude in the orbital reference frame (roll and pitch angles).

Usually Earth sensors detect infrared radiation emitted from the Earth's surface. They can be used in sunlight and during eclipse but the presence of the Sun or the Moon in the FoV introduces disturbances. Also, Earth oblateness contributes to the attitude determination uncertainty.

Two types of sensors are used — static and scanning Earth sensors. For static Earth sensors, the Earth has to be in the FoV permanently. To determine attitude around two axes, two or more sensors have to be used. Scanning Earth sensors either rotate themselves or the whole satellite spins. A rotating

sensor sweeps out a cone and determines the attitude from signals generated when the Earth's horizon enters and leaves the FoV. [58]

3.2.4   Star trackers

Star trackers determine attitude by identifying star patterns. They are the most complex attitude sensors with high computational requirements but, at the same time, the most accurate ones. There are multiple reasons why star trackers are so accurate (below $0.1°$). First, the apparent size of stars is small, hence direction can be determined with high precision. Second, stars are inertially fixed, hence determining attitude in the ECI frame does not require additional models and attitude transformations. Third, sensors can track multiple stars, hence minimise the measurement uncertainty and determine the attitude from one sample. A star tracker alone can be used as a three-axis attitude determination system.

Since star trackers essentially are imagers of objects with low brightness, the required exposure time limits the spin rate a spacecraft can have. Also, the Sun and the Earth cannot be in the FoV of a star tracker. While star trackers work as three-axis attitude determination systems, they are usually used together with other attitude determination sensors due to the fact that processing an image for attitude determination takes a significant amount of time and computational resources. Hence, intermediate attitude is propagated by angular velocity measurements or determined by another method. Due to optics and a baffle, star trackers are usually the heaviest sensors compared with other attitude sensors. The baffle is required to avoid stray light from the Earth and the Sun. [58]

3.2.5   Angular velocity sensors

Angular velocity sensors measure the spin rate of a satellite in an inertial reference frame. Although spin rate can be determined from other attitude measurements by differentiation, measuring the spin rate directly provides lower noise level without having to consider the orbital motion of the satellite (satellite moving with respect to an external reference).

As opposed to other sensors discussed in this section, angular velocity sensors provide measurements independent of an external reference. This property allows the taking of measurements without the Sun, the Earth or stars in the FoV, or outside the Earth's magnetosphere. For example, angular velocity measurements are especially useful to propagate the attitude while the satellite is in the eclipse. However, angular velocity measurements are biased,

in addition to noise and gain error, and the attitude propagated using angular velocity will drift.

The bias is a non-zero sensor output at 0 deg·s^{-1} rotation rate with respect to an inertial reference frame. While the bias can change over time and after turning the sensor off and on, it is also influenced by the temperature, magnetic field, acceleration and other factors. The gain converts raw sensor readings to angular velocity. The gain is also influenced by the temperature, hence it is important to include the temperature effects when calibrating angular velocity sensors. While the noise level is usually low for angular velocity sensors, it can have a significant contribution when angular velocity measurements are used to propagate the attitude. Due to this, filtering can be used, especially for miniaturised sensors for which the noise level might be fairly high. [58]

Historically, mechanical gyroscopes were used to measure the angular velocity but recently laser gyroscopes have become popular due to the benefit of no moving parts [56]. On nanosatellites, COTS micro-electro-mechanical systems based vibratory systems for angular velocity sensors are used [62].

3.2.6 ESTCube-1 attitude sensor set

The main considerations for choosing attitude determination sensors for ESTCube-1 are the ability to provide reliable measurements when the satellite spins with the rate of one rotation per second, as well as the mass, volume and power consumption.

Star trackers and Earth sensors are excluded from selection due to significant mass contributions by optics and a baffle. In addition, since the satellite is spinning around the axis that is aligned with the Earth's polar axis, Earth sensors would not be able to provide attitude measurements throughout the orbit. Star trackers are also limited by the maximum spin rate at which they are able to operate. The maximum limit is usually of an order of magnitude of 10 deg·s^{-1}. The advantage of analogue Sun sensors over digital ones is simplicity and low power requirements due to the fact that analogue PSDs are passive detectors — they generate photocurrent from sunlight. They are also not limited by the spin rate of the satellite because a continuous signal is provided by the PSD and it can be read instantaneously. Nevertheless, the performance is limited by the Analogue to Digital Converter (ADC) sampling rate.

The following set of sensors was chosen for ESTCube-1 — analogue Sun sensors, magnetometers and gyroscopic sensors. Since, at the time of designing the system, suitable Sun sensors were not available commercially, ESTCube-1 Sun sensors were developed in-house. While the selected set of sensors is op-

timal for ESTCube-1, the system has certain limitations, namely, Sun sensors cannot be used in the eclipse, Sun sensors have to be placed on all sides of the satellite to maximise the FoV, the attitude determination uncertainty will increase when using angular velocity measurements to propagate the attitude during the eclipse, and magnetometer measurements cannot be taken at the same time when magnetorquers are used.

3.3   Reference models

Reference models are used to reference sensor measurements. Since ESTCube-1 is using Sun sensors and magnetometers, the Sun position model and the Earth magnetic field model are required. In order to use the Earth magnetic field model, position of the satellite and the rotation of the Earth have to be known.

3.3.1   Orbital perturbation model

Modelling of orbits is not directly related to attitude determination but for many missions the orbital position of the satellite is required in order to determine the attitude. For example, when magnetic field measurements are referenced to the geomagnetic field model this requires orbital position as an input to calculate the magnetic field vector.

An idealised orbital equation, the Keplerian two-body orbital equation, is derived from the Newton's laws of motion and the Newton's law of gravitation. It is presented in Equation 3.1, where $\mathbf{r}$ is the position vector of the satellite, G is the universal gravitational constant and m is the mass of the body that the satellite is orbiting around (assuming that mass of the orbiting body is $\ll m$). A point mass approximation is used here. [56]

$$\ddot{\mathbf{r}} = -\frac{Gm}{|\mathbf{r}|}\mathbf{r} \tag{3.1}$$

Orbits are described by orbital elements, for example, Keplerian elements. The eccentricity defines the shape of an orbit, the semimajor axis define the size, the orientation of the orbital plane is defined by the inclination and the longitude of the ascending node, the orientation of the ellipse in the orbital plane is defined by argument of periapsis, and the mean anomaly at epoch defines the position of the satellite in an orbit.

Orbital perturbations play a significant role in determining an orbit and the position of a satellite. Satellites in the Earth's orbit are affected by the following perturbations. First, the Earth is not perfectly spherical, hence

the point mass approximation is not precise. Second, other bodies influence the orbit, for example, the Sun and the Moon. Third, in low Earth orbits, the atmospheric drag decreases the orbital velocity. Fourth, solar radiation pressure transfers the momentum from photons to the satellite surface. [56]

In practise, orbital elements, not necessarily Keplerian elements, are determined using measurements (e.g., radar, laser ranging or Doppler shift measurements). While the theoretical background on orbital perturbations is wide, it is not in the scope of this thesis and here just a practical method used on ESTCube-1 will be discussed briefly.

One of the most widely used set of orbital elements, especially when high accuracy is not required, is the North American Aerospace Defense Command (NORAD) element set (also known as the Two-Line Element set, TLE) [63]. The NORAD element set works with five satellite position prediction models: Simplified General Perturbations (SGP) [64], SGP4 [65], Simplified Deep space Perturbations (SDP4) [66], SGP8 [67] and SDP8 (based on SGP8). SGP models are used with orbital periods smaller than 225 minutes and SDP models with periods larger than that. The orbital period of 225 minutes corresponds to a circular orbit of about 5877 km altitude. All models with FORTRAN code are provided in [63]. The TLE consists of the following elements and administrative fields: NORAD catalogue number, security classification, launch year, number and piece letter, epoch year and day (including fractional hours) of the orbital element, first time derivative of the mean anomaly, atmospheric drag term, ephemeris (model) type, element number, inclination, right ascension of ascending node, eccentricity, argument of the perigee, mean anomaly, mean motion and revolution number at epoch.

While the error in the predicted position can be tens of kilometres [68], due to its simplicity and availability of TLEs, the SGP4 model is widely used. In the case of ESTCube-1, the orbital position uncertainty is 3.5 km and contributes $0.1°$ to the uncertainty budget (standard uncertainties) [**IV, Table 1**].

3.3.2   Earth rotation model

The Earth rotation model calculates the rotation between the ECI frame and the ECEF, using the time as an input. One rotation of the Earth corresponds to the mean Sidereal day of 23 hours, 56 minutes and 4.09053 seconds [69]. The reference time for the Earth's rotation is the Greenwich meridian transit of the equinox on December 31, 1996 at 17 hours, 18 minutes and 21.8256 seconds. From the reference time, full rotations are calculated and the fractional part corresponds to the Earth's rotation that day. The model is based on the work

by Princeton Satellite Systems, Rafał Wiśniewski (Aalborg University) and the final version was prepared for the AAUSAT3 satellite [53].

The Earth rotation model does not account for precession and nutation, hence they contribute to the uncertainty budget [**IV, Table 1**]. Precession contributes $0.15°$ and nutation contributes $0.0015°$ to the uncertainty budget (standard uncertainties) [52]. The contribution by precession could have been minimised by using a later reference time but, unfortunately, such improvement was not included in on-board software.

3.3.3   Geomagnetic field model

The geomagnetic field or the magnetic field of the Earth is the magnetic field generated by the motion of conductive fluids in the Earth's core [70]. While the processes generating the geomagnetic field are not fully understood, it can be measured, modelled and predicted. Multiple models of the geomagnetic field have been developed and their coefficients are usually updated every five years using ground and satellite measurements. Examples of these models are CHAMP, Ørsted and Swarm (CHAOS) [71], the International Geomagnetic Reference Field (IGRF) [72], the World Magnetic Model (WMM) [73], and the Canadian Geomagnetic Reference Field (CGRF) [74].

The latest IGRF generation is the 12th but on ESTCube-1 the 11th generation IGRF, valid for 1900–2015, was used [75]. The magnetic field was calculated using a simple C implementation suitable for running on board the satellite [53; 76]. By using harmonic series and data from CHAMP and Ørsted satellites, as well as from magnetic field observatories, the IGRF models the main magnetic field and secular variations. Since the magnetic field of the Earth is changing, every five years the coefficients are updated and the model is assumed to be linear over a five year period. When calculating the magnetic field vector, in addition to position in the ECEF, the time has to be specified.

Since 2000, the IGRF uses order 13 harmonics to better represent measurement data. Nevertheless, the standard deviation of the magnetic field is about 100 nT due to temporal changes in the magnetic field [76; 77]. Geomagnetic field uncertainty contributes $0.42°$ to the attitude determination uncertainty budget [**IV, Table 1**].

3.3.4   Sun position model

The Sun position model is a simple function that takes time as an input and outputs the position of the Sun. In the implementation used on ESTCube-1 [78], originally the Julian date was used as an input together with the space-

craft position vector in the ECI frame. However, on-board code was modified to use the ESTCube-1 time as an input. The ESTCube-1 time is a timestamp that started on 21.12.2012 00:00:00 and uses steps of 100 ms. The model calculates the mean anomaly, the obliquity of ecliptic, and uses the spacecraft position vector to account for parallax. The model outputs a normalised position vector of the Sun in the ECI frame, as well as the distance to the Sun. Despite its simplicity, the accuracy of the model is one minute of arc, which contributes to the uncertainty budget [**IV, Table 1**].

3.4   Attitude estimation

Knowing sensor measurements in the SBRF (Section 3.2), the spacecraft position and reference vectors in the ECI frame (Section 3.3), the goal is to estimate the orientation of the SBRF in the ECI frame. Estimation can be performed by batch approach or Kalman filtering. The batch approach uses a set of measurements taken at the same time. The most popular batch approach algorithms are TRIAD (also known as the Algebraic Method) [79; 80], q-method [81] and Quaternion Estimator [82; 83]. Quaternions are rotation formalism widely used in spacecraft attitude determination. Their main advantage is that trigonometric functions are not required, they are free from singularities and are very suitable for computers due to low computational requirements and algebraic operations [52; 56; 84].

   With increasing computational power on board satellites, a more sophisticated method for attitude estimation, the Kalman filter [85], has become popular. The Kalman filter was also chosen for ESTCube-1 due to having enough processing power to run it on board. The method takes advantage of historical measurements, it uses not only direction and position measurements (like magnetic field vector and Sun vector) but also angular velocity measurements, it employs spacecraft kinematic and dynamic models, as well as takes into account knowledge about measurement covariance. In the case that the system is overdetermined, the Kalman filter can also estimate the measurement bias. Generally, the Kalman filter consists of initialisation, prediction and correction steps.

   For ESTCube-1, an Unscented Kalman Filter (UKF) originally developed for the AAUSAT3 satellite was used [40]. The UKF combines the extended Kalman filter with a set of sigma points that are used to approximate the Gaussian probability distribution of the input and the output. The extended Kalman filter is a suitable variant of the Kalman filter for attitude estimation since the filter linearises the model. The UKF is based on a sigma point sam-

pling method called unscented transform. Sigma points are a structured set of sample points selected in such a way that they give adequate coverage of the input and output probability distribution. The UKF implementation makes the initial attitude guess by solving the Wahba's problem [86] using the singular value decomposition method. Since the filter propagates the attitude using angular velocity measurements, knowledge of the moment of inertia matrix is required. It is especially important when performing attitude estimation at high spin rates. [87; 88]

3.5 System design

Historically, for large satellites, attitude determination sensors are of a size comparable with the size of nanosatellites. For example, a star tracker developed for missions in geostationary orbit weighing more than 6 kg [89], fine Sun sensors weighing 0.6 kg [90], an Earth sensor weighing 3.5 kg [91], gyroscopic sensors weighing 450 g per axis [92], and magnetometers weighing about 0.5 kg [58]. In order to equip ESTCube-1 with an attitude determination system, the sensor mass has to be decreased by between one and two orders of magnitude. This has been achieved by employing COTS consumer electronics components.

A diagram of the ESTCube-1 ADS is presented in Figure 3.2. The system consists of a sensor board and Sun sensors located on all sides of the satellite. The ADS is connected with the Command and Data Handling System (CDHS) where calculations are executed. The sensor board contains two Honeywell HMC5883L magnetometers [93], four Invensense ITG-3200 gyroscopic sensors [94] and two Maxim MAX1230 ADCs [95] to which Sun sensors are connected. ADCs also have built-in temperature sensors. Sun sensors are based on two Hamamatsu S3931 PSDs [96] located under a mask with two slits perpendicular to each PSD. The mass of each sensor is 4.6 g and each consumes 4 mW. Together with ADCs the average power consumption of Sun sensors is 96 mW. Magnetometers and gyroscopic sensors are connected to the CDHS with two inter-integrated circuit bus interfaces. Each interface is connected to a couple of gyroscopic sensors and one magnetometer. ADCs are connected to the CDHS via a serial peripheral interface. By executing calculations on the CDHS, the total mass of the system was reduced, and redundancy provided by the CDHS was employed. An STMicroelectronics STM32F103 processor is used on the CDHS. All sensor measurements are pre-processed — faulty measurements (e.g., zero magnetic field vector or out-of-range values) are discarded, and filters and weights are applied. Sensors are calibrated and corrected for zero offsets and temperature influences. Sensor

measurements together with outputs of the Sun direction model, the satellite position model and the magnetic field model are given to the UKF. Measurement noise covariances are also given to the UKF, which outputs the attitude, the estimated magnetic field and the estimated angular velocity. Estimated values are based on bias estimation results. [**III**]
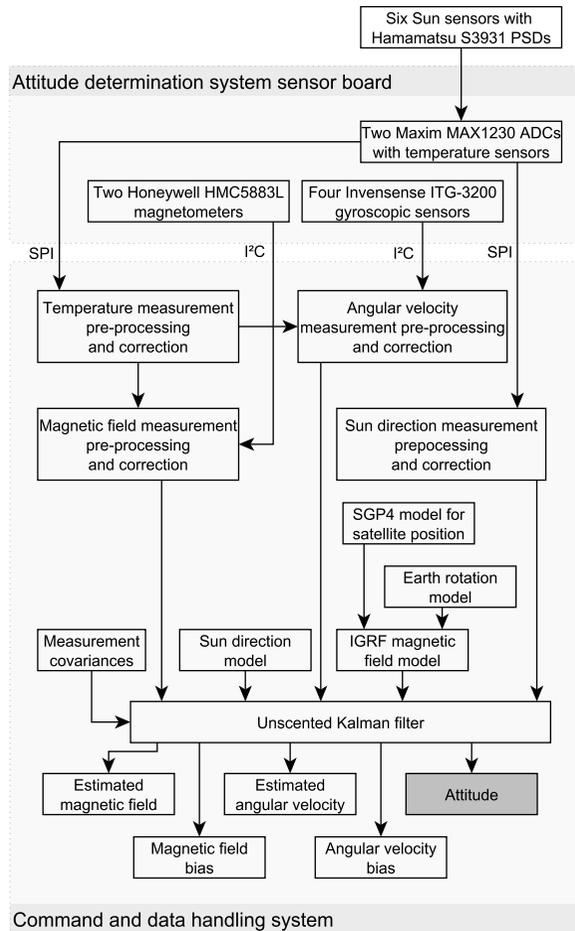
Figure 3.2: ESTCube-1 attitude determination system diagram. I^{2}C — Inter-Integrated Circuit, SPI — Serial Peripheral Interface.

Chapter 4
Characterisation and validation

The designed ADS (Section 3.5) was first characterised by laboratory measurements and simulations. After launching the satellite, the system performance was analysed and software was developed and tuned to improve the performance. The system was validated by using an independent attitude determined from on-board images.

4.1   Characterisation

The system was developed and characterised by laboratory tests and simulations. For evaluation of the uncertainty of the result, recommendations from the standard guide "Evaluation of measurement data — Guide to the expression of uncertainty in measurement" are followed [59].

The average power consumption of the sensor board at full load is 262 mW; for the CDHS board — 178 mW. Both boards are built to be used in a CubeSat and the size is $92 \times 94 \times 5$ mm. The combined mass of the sensor board and Sun sensors is 45 g; the mass of the CDHS board is 49 g. One iteration of attitude determination calculations (taking measurements, processing of measurements, running reference models and the UKF) takes less than 150 ms when the processor clock frequency is set to 32 MHz with 72 MHz being the maximum clock frequency. [**III**]

The expanded uncertainty for the angle of incident light measured by the Sun sensor is $2.5°$ [**III, Section 4**]. The following factors contribute to the uncertainty budget: the albedo of the Earth (standard uncertainty of $1°$), the temperature ($0.76°$), the solar irradiance uncertainty ($0.25°$), the testing equipment precision ($0.081°$), the resolution ($0.02°$) and the noise ($0.005°$). The expanded uncertainty of the direction of the angle of the magnetic field is $3.2°$ [**III, Section 5**]. The following factors contribute to the uncertainty budget: the temperature (standard uncertainty of $1.4°$), the noise ($0.8°$) and the testing equipment precision ($0.3°$). The expanded uncertainty for the angular velocity is 3.6 deg·s^{-1} [**III, Section 6**]. The following factors contribute to the uncertainty budget: the temperature (standard uncertainty of 1.5 deg·s^{-1}), the noise (0.9 deg·s^{-1}), the influence of the vacuum (0.2 deg·s^{-1}), the testing equipment precision (0.1 deg·s^{-1}) and the resolution (0.07 deg·s^{-1}). While uncertainties of sensors separately are bigger than the required attitude determination accuracy, the measurements are still to be processed and fused by

the UKF in order to estimate the attitude and angular velocity determination accuracy.

Attitude determination with conditions that were expected during the experiment were simulated — a spin rate of about 20 deg·s^{-1} around the z-axis, and the spin axis nearly aligned with the Earth's polar axis. To estimate the ability of the system to determine the attitude with the required accuracy, the following factors were simulated: radiation; atmospheric, gravity and magnetic residual disturbances; the time bias; biases for all sensors; the Gaussian noise for all measurements (values taken from sensor uncertainty budgets); tilting of the magnetometer and the gyroscopic sensor; variations in the inertia matrix knowledge; and variations in the measurement noise covariance for the UKF.

The expanded uncertainty (95% confidence level, $k = 2$) of attitude determination is 1.52° [**IV, Table 1**]. The uncertainty budget includes the simulation-based uncertainty estimated by standard deviation (0.6°), the geomagnetic field model uncertainty (0.42°), the Earth precession uncertainty (0.15°), the orbit propagation uncertainty (0.1°), the Earth nutation uncertainty (0.01°), and the modelled Sun direction uncertainty (0.0015°).

4.2   In-orbit performance

After the ESTCube-1 launch, ADS software was improved and updated and the system was tuned. The sequence of attitude determination and control tasks was improved to maximise frequency of attitude control. Measurement noise covariances were estimated. Sensor performance was analysed and software was developed to avoid using low-accuracy or faulty measurements. The moment of inertia matrix was estimated based on in-orbit measurements to improve attitude estimation.

The timeline of attitude determination and control sequence was improved by executing attitude determination tasks in parallel with attitude control of magnetic moment calculated in the previous iteration. To avoid faulty magnetic field measurements, electromagnetic coils were not used when measurements were taken. Such an approach and code optimisation enabled the running of the attitude determination and control sequence with a frequency more than 10 Hz provided that the processor was run with the highest clock frequency of 72 MHz. For a high spin rate of the satellite, timing is critical — the determined attitude is extrapolated to the moment when the attitude control is to be executed. This approach proved to be successful, since the satellite was able to reach a spin rate of 2.4 rotations per second [47].

By minimising the error between the attitude determined by the ADS

and from on-board images, measurement noise covariances for the UKF were estimated iteratively. The magnetic field vector direction noise covariance is 2.4×10^{-7} rad. The angular velocity measurement noise covariance is 6×10^{-6} rad·s^{-1}. The Sun sensor covariance varies depending on the incidence angle — it increases when the incidence angle approaches the limit of the FoV. The FoV was limited to $\pm 36.7°$ in software and the measurement noise covariance was set to 1.75×10^{-6} rad for the FoV of $\pm 20°$. Between the FoV $\pm 20°$ and $\pm 36.7°$, the measurement noise covariance is quadratically increased to 0.01 rad. When the Sun is not in the FoV, the UKF runs as in the eclipse. Such an approach was also used when the Sun illuminates the side of the satellite on which the Sun sensor was broken. The most probable cause of the broken sensor was a loose wire. A few weeks after the launch one of the gyroscopic sensors started to malfunction. That, however, did not cause any problems because there are four gyroscopic sensors on the ADS board. [**IV**]

Re-estimation of the moment of inertia matrix was required because the one provided by the computer aided design model was not precise enough to effectively estimate the attitude at high spin rates. The inertia matrix was found by minimising differences between the uncontrolled rotation of the satellite in orbit and the simulated rotation. The moment of inertia matrix was chosen such that rotations match. The matrix consists of the following elements:

$$10^{-3} \cdot \begin{bmatrix} 2.25242 & 0.02109 & 0.03208 \\ 0.02109 & 2.45397 & 0.03730 \\ 0.03208 & 0.03730 & 2.24506 \end{bmatrix} \text{kg} \cdot \text{m}^2.$$

4.3 Validation

To validate the ADS, an independent attitude determined from on-board images was used. The on-board camera has a 4.4 mm telecentric lens and a 640×480 pixel complementary metal-oxide semiconductor sensor [97]. The attitude is extracted from images in post-processing. A set of coordinates of well distinguishable landmarks in the image coordinate system, as well as corresponding points on the map with a geographical coordinate system were selected to determine the attitude from images. Similar to the ADS, time and orbital elements were required to calculate the orbital position. Points were selected such that the system is overdetermined and the attitude is determined by minimising the angular difference between two sets of camera space vectors.

The expanded uncertainty (95% confidence level, $k = 2$) of the image-based attitude determination is $0.86°$ [**IV, Table 2**]. The uncertainty budget

includes the point selection uncertainty (standard uncertainty: $0.37°$), the time uncertainty ($0.21°$), the camera resolution uncertainty ($0.04°$) and the lens distortion uncertainty ($0.02°$). The expanded uncertainty of comparison (95% confidence level, $k = 2$) is $1.75°$. This value is calculated by combining the uncertainty of ADS attitude determination (Section 4.1) and the uncertainty of image-based attitude determination.

Differences between the attitude determined by both methods were calculated for 15 samples. Images were taken during attitude determination sessions. For all samples the difference is smaller than $1.44°$, which is well within the uncertainty budget [**IV, Table 3**]. The results indicate that the ADS fulfils the mission requirement to determine the attitude with an accuracy better than $2°$.

Chapter 5
Discussion and conclusions

This thesis presents the ESTCube-1 attitude determination system. The main objective of the system is to serve the electric solar wind sail experiment. The system is required to determine the attitude of ESTCube-1 with an accuracy better than 2°. The attitude is used for the following: as an input for high rate spin control (hundreds of degrees per second) required for centrifugal electric solar wind sail tether deployment; for monitoring tether deployment; in order to determine the timing of the charging of the tether in synchronisation with the satellite spin; and for measuring changes in the angular velocity caused by the Coulomb drag interaction between the charged tether and the surrounding plasma. The experiment was planned to be performed over the poles and it was estimated that during one polar pass the change of angular rate would be ≈ 0.5 deg·s^{-1}. Preliminary requirements for attitude determination sensors were set by simulating high rate spin control.

In order to employ the one-unit CubeSat standard, the volume was the main design driver. For the attitude determination system, a set of sensors was chosen that would have the smallest size. The system has Sun sensors, magnetometers and gyroscopic sensors. Sun sensors are custom-built and placed on all sides of the satellite. For all sensors, commercially available consumer electronics components were used. Sensor measurements with outputs from the geomagnetic field model and the Sun position model are given to the unscented Kalman filter for attitude estimation.

To provide reliable attitude measurements, sensors and the whole attitude determination system were characterised in the laboratory and by simulations. The expanded uncertainty (95% confidence level, $k = 2$) for Sun sensors is 2.5°, for gyroscopic sensors — 3.6 deg·s^{-1}, for magnetometers (magnetic field direction) — 3.2°. While the sensor uncertainties are high when compared with the required attitude determination accuracy, simulations showed that the unscented Kalman filter estimates the attitude with a standard deviation of 0.6° for parts of the orbit where the electric solar wind sail experiment was planned to be performed. In addition to the simulation-based standard uncertainty, the following standard uncertainty contributors were included in the uncertainty budget for the attitude determination system — the geomagnetic field model uncertainty (0.42°), the Earth's precession (0.15°), the orbit propagator uncertainty (0.1°), the Earth's nutation (0.01°), and the Sun direction model uncertainty (0.0015°). The combined expanded uncertainty of attitude

determination is 1.52°.

The system was validated in orbit by using an independent attitude determined from on-board images. The following standard uncertainty contributors were included in the uncertainty budget for image-based attitude determination — the point selection uncertainty (0.37°), the time uncertainty (0.21°), the resolution uncertainty (0.04°), and the lens distortion uncertainty (0.02°). The combined expanded uncertainty of image-based attitude determination is 0.86°.

The system fulfils the requirement, set by the electric solar wind sail experiment, to determine the attitude better than 2° — the expanded uncertainty of comparison is 1.75°. For all 15 samples used to compare results from both attitude determination methods, the difference is less than 1.44°, which is well within the uncertainty budget.

The ESTCube-1 project achieved the objective to provide hands-on education and to popularise science. More than 200 students were involved in the project as developers, team leaders and managers. The senior staff had an advisory role in the project. Students wrote more than 30 bachelor theses and more then 20 master theses, published more than ten journal articles, eight conference papers, presented seven posters, gave more than 50 technical presentations, participated in ten workshops and seminars, wrote more than ten popular science articles and gave more than 30 popular science talks and interviews. The project provided a unique opportunity for more than 20 secondary school pupils to contribute to the mission during summers.

By building, launching and operating the satellite, the team learned lessons that would have otherwise not been possible. Although tether deployment was not successful [47], the best practises and lessons learned have been and are implemented on follow-up missions Aalto-1 [48] and ESTCube-2.

In the future, the following is suggested to improve attitude determination. Sun sensor measurements can be improved by increasing the field of view, by correcting for temperature effects, by avoiding unwanted reflections inside the mask, and by modelling the Earth's albedo. Magnetometer performance can be improved by avoiding residual magnetic moment on board the satellite. All sensor measurements can be improved by rotating around an arbitrary axis during calibration and by having more temperature and voltage references. Attitude estimation can be improved by having a good knowledge of the inertia matrix. It is especially important when using a Kalman filter which includes a prediction step and when performing high spin rate manoeuvres. ESTCube-1 had the functionality to update software in orbit. It proved to be beneficial for troubleshooting, updating, and in-orbit characterisation of the attitude

determination system. [47]

While consumer electronics commercial off-the-shelf components have been used on satellites only in the last 15 years, and such systems are still looked at sceptically, reliable systems can be developed by carefully characterising components and sensors, and by implementing redundancy. In turn, such an approach provides affordable access to space due to low mass, utilises the latest developments in consumer electronics and enables rapid developments for technology demonstration.

Summary

This research was carried out at the University of Tartu, Tartu Observatory, the Finnish Meteorological Institute and the Estonian Student Satellite Programme. This thesis presents the ESTCube-1 attitude determination system. The attitude is the satellite's orientation is space. ESTCube-1 is a satellite built according to the one-unit CubeSat standard ($\approx 10 \times 10 \times 10$ cm). The satellite was launched in May 2013 and operated until May 2015. The main scientific mission of ESTCube-1 was to perform the first in-orbit electric solar wind sail demonstration. The electric solar wind sail is a propellantless propulsion technology concept. The sail consists of long, thin, centrifugally stretched and positively charged tethers that deflect charged particles in the solar wind, hence generate spacecraft thrust.

The main requirement of the ESTCube-1 attitude determination system is to determine the attitude with an accuracy better than $2°$ for the following purposes: high rate spin control (hundreds of degrees per second) for centrifugal tether deployment; monitoring of tether deployment; to trigger the charging of the tether in synchronisation with the satellite spin; to measure angular velocity changes caused by the Coulomb drag interaction between the charged tether and the surrounding ionospheric plasma.

The attitude determination system has Sun sensors, magnetometers and gyroscopic sensors. A geomagnetic field model and a Sun position model were used to reference the respective sensor measurements. A Kalman filter was used to estimate the attitude. Before the launch, the system was characterised in the laboratory and by simulations. With in-orbit recalibration and validation, the system was significantly improved. For validation, an independent attitude determined from on-board images was used. By characterising and validating the system, it was shown that attitude determination accuracy is better than $1.75°$, hence fulfils the requirement set by the electric solar wind sail experiment.

Kokkuvõte (Summary in Estonian)

ESTCube-1 asendi määramine

Uuring viidi läbi Tartu Ülikoolis, Tartu Observatooriumis, Soome Meteoroloogia instituudis ja Eesti tudengisatelliidi programmis. Doktoritöös tutvustatakse satelliidi ESTCube-1 asendi määramise süsteemi, mille otstarve on satelliidi orientatsiooni kindlakstegemine erinevate taustsüsteemide suhtes. ESTCube-1 on ehitatud vastavalt CubeSat standardi nõuetele (≈ 10 cm $\times$ 10 cm $\times$ 10 cm) ja saadeti orbiidile 2013. aasta mais, kus see tegutses kuni 2015. aasta maini. Selle põhimissiooniks oli katsetada Maa orbiidil elektrilise päikesepurje tehnoloogiaid. Elektriline päikesetuulepuri on uudne Päikesesüsteemis liikumise moodus, mis kasutab tõukejõu saamiseks Päikeselt väljapursatavate elektriliselt laetud osakeste voogu ehk päikesetuult.

ESTCube-1 asendi määramise süsteemi põhieesmärgiks on leida satelliidi orientatsioon parema täpsusega kui 2° järgmiste tegevuste jaoks: satelliidi suure kiirusega pöörlema panemisel (sajad kraadid sekundis) tsentrifugaaljõu abil purje väljakerimiseks ja selle protsessi jälgimiseks, päikesepurje elektrilisel laadimisel sünkroonis satelliidi pöörlemisega ning mõõtmaks nurkkiiruse muutumist laetud päikesepurje ja ionosfääri plasma vahelise elektrostaatiline jõu tulemusel.

Asendi määramise süsteem koosneb magnetomeetridest, nurkkiiruseanduritest ja Päikese suuna anduritest. Maa magnetvälja ja Päikese asukoha mudeleid kasutati vastavate andurite mõõtmistega võrdlemiseks. Asendi määramiseks kasutati Kalmani filtrit. Süsteem karakteriseeriti laboratooriumis ja simulatsioonidega enne starti. Orbiidil parendati süsteemi oluliselt tarkvara uuenduste ja uuesti karakteriseerimisega. Sõltumatuks valideerimiseks kasutati satellidi poolt tehtud fotodel põhinevat orientatsiooni leidmise meetodit. Süsteemi karakteriseerimise ja valideerimisega näidati, et asendi määramise täpsus on parem kui 1.75° mis täidab eksperimendi poolt seatud nõudeid.

References

[1] F. A. Zander, "Flights to other planets," *Tekhnika i Zhizn*, vol. 13, pp. 15–16, 1924.

[2] H. J. Oberth, *Ways to spaceflight*. Verlag, 1929.

[3] K. E. Tsiolkovsky, "Extension of man into outer space," in *Proceedings of the Symposium on Jet Propulsion*, 1936.

[4] J. Verne, *From the Earth to the Moon*. Pierre-Jules Hetzel, 1863.

[5] R. L. Garwin, "Solar sailing — a practical mothod of propulstion within the Solar System," *Jet Propulsion*, vol. 28, pp. 188–190, 1958.

[6] M. Macdonald and C. McInnes, "Solar sail science mission applications and advancement," *Adv. Space Res.*, vol. 48, pp. 1702–1716, 2011.

[7] L. Johnson, R. Young, N. Barnes, L. Friedman, V. Lappas, and C. McInnes, "Solar sails: Technology and demonstration status," *Int'l J. of Aeronautical & Space Sci.*, vol. 13, no. 4, pp. 421–427, 2012.

[8] D. G. Andrews and R. M. Zubrin, "Magnetic sails and interplanetary travel," *J. Spacecr. Rockets*, vol. 28, pp. 197–203, 1991.

[9] R. M. Winglee, J. Slough, T. Ziemba, and A. Goodson, "Mini-magnetospheric plasma propulsion tapping the energy of the solar wind for spacecraft propulsion," *J. Geophys. Res.*, vol. 105, pp. 21 067–21 077, 2000.

[10] P. Janhunen, "Electric sail for spacecraft propulsion," *J. Propul. Power*, vol. 20, pp. 763–764, 2004.

[11] P. Janhunen and A. Sandroos, "Simulation study of solar wind push on a charged wire: basis of solar wind electric sail propulsion," *Ann. Geophys.*, vol. 25, pp. 755–767, 2007.

[12] P. Janhunen, P. K. Toivanen, J. Polkko, S. Merikallio, P. Salminen, E. Hæggström, H. Seppänen, R. Kurppa, J. Ukkonen, S. Kiprich, G. Thornell, H. Kratz, L. Richter, O. Krömer, R. Rosta, M. Noorma, J. Envall, S. Lätt, G. Mengali, A. A. Quarta, H. Koivisto, O. Tarvainen, T. Kalvas, J. Kauppinen, A. Nuottajärvi, and A. Obraztsov, "Electric solar wind

sail: Toward test missions," *Rev. Sci. Instrum.*, vol. 81, pp. 111 301:1–11, 2010.

[13] P. Janhunen, P. Toivanen, J. Envall, S. Merikallio, G. Montesanti, J. G. del Amo, U. Kvell, M. Noorma, and S. Lätt, "Overview of electric solar wind sail applications," *Proc. Estonian Acad. Sci.*, vol. 63(2S), pp. 267–278, 2014.

[14] A. A.Quarta, G. Mengali, and P. Janhunen, "Optimal interplanetary rendezvous combining electric sail and high thrust propulsion system," *Acta Astronaut.*, vol. 68, pp. 603–621, 2011.

[15] A. A.Quarta and G. Mengali, "Electric sail missions to potentially hazardous asteroids," *Acta Astronaut.*, vol. 66, pp. 1506–1519, 2010.

[16] S. Merikallio and P. Janhunen, "Moving an asteroid with electric solar wind sail," *Astrophys. Space Sci. Trans.*, vol. 6, pp. 41–48, 2010.

[17] G. Mengali and A. A. Quarta, "Non-Keplerian orbits for electric sails," *Celest. Mech. Dyn. Astr.*, vol. 105, pp. 179–195, 2009.

[18] M. Ceriotti, B. L. Diedrich, and C. R. McInnes, "Novel mission concepts for polar coverage: An overview of recent developments and possible future applications," *Acta Astronaut.*, vol. 80, pp. 89–104, 2012.

[19] P. Janhunen, S. Merikallio, and M. Paton, "EMMI — Electric solar wind sail facilitated Manned Mars Initiative," *Acta Astronaut.*, vol. 113, pp. 22–28, 2015.

[20] P. Janhunen, "Electrostatic plasma brake for deorbiting a satellite," *J. Propul. Power*, vol. 26, pp. 370–372, 2010.

[21] ——, "Simulation study of the plasma brake effect," *Ann. Geophys.*, vol. 32, pp. 1207–1216, 2014.

[22] "Electric sail propulsion technology," Finnish Meteorological Institute, Final Report of FP7 Project, 2013.

[23] *European Cooperation for Space Standardization, ECSS-E-ST-10C, Space engineering: System engineering general requirements*, European Space Agency Std.

[24] H. Seppänen, S. Kiprich, R. Kurppa, P. Janhunen, and E. Hæggström, "Wire-to-wire bonding of μm-diameter aluminum wires for the electric solar wind sail," *Microelectron. Eng.*, vol. 88, pp. 3267–3269, 2011.

[25] H. Seppänen, T. Rauhala, S. Kiprich, J. Ukkonen, M. Simonsson, R. Kurppa, P. Janhunen, and E. Hæggström, "One kilometer (1 km) electric solar wind sail tether produced automatically," *Rev. Sci. Instrum.*, vol. 84, pp. 095 102:1–4, 2013.

[26] J. Envall, P. Janhunen, P. Toivanen, M. Pajusalu, E. Ilbis, J. Kalde, M. Averin, H. Kuuste, K. Laizāns, V. Allik, T. Rauhala, H. Seppänen, S. Kiprich, J. Ukkonen, E. Haeggström, T. Kalvas, O. Tarvainen, J. Kauppinen, A. Nuottajärvi, and H. Koivisto, "E-sail test payload of ESTCube-1 nanosatellite," *Proc. Estonian Acad. Sci.*, vol. 63(2S), pp. 210–221, 2014.

[27] R. Rosta, O. Krömer, T. v. Zoest, P. Janhunen, and M. Noorma, "Wrecker: an unreeling mechanism for a thin electrically conductive space tether," *CEAS Space J.*, vol. 7(1), pp. 53–68, 2015.

[28] J. Bouwmeester and J. Guo, "Survey of worldwide pico- and nanosatellite missions, distributions and subsystem technology," *Acta Astronaut.*, vol. 67, no. 7-8, pp. 854–862, 2010.

[29] K. Woellert, P. Ehrenfreund, A. J. Ricco, and H. Hertzfeld, "Cubesats: Cost-effective science and technology platforms for emerging and developing nations," *Adv. Space Res.*, vol. 47, pp. 663–684, 2011.

[30] W. A. Shiroma, L. K. Martin, J. M. Akagi, J. T. Akagi, B. L. Wolfe, B. A. Fewell, and A. T. Ohta, "CubeSats: A bright future for nanosatellites," *Central European Journal of Engineering*, vol. 1, pp. 9–15, 2011.

[31] M. Ansdell, P. Ehrenfreund, and C. McKay, "Stepping stones toward global space exploration," *Acta Astronaut.*, vol. 68, no. 11-12, pp. 2098–2113, 2011.

[32] D. Selva and D. Krejci, "A survey and assessment of the capabilities of Cubesats for Earth observation," *Acta Astronaut.*, vol. 74, pp. 50–68, 2012.

[33] P. Ehrenfreund, C. McKay, B. H. F. John D. Rummel, C. R. Neal, T. Masson-Zwaan, M. Ansdell, N. Peter, J. Zarnecki, S. Mackwell, M. A. Perino, L. Billings, J. Mankins, and M. Race, "Toward a global space exploration program: A stepping stone approach," *Adv. Space Res.*, vol. 49, no. 1, pp. 2–48, 2012.

[34] M. Swartwout, "The first one hundred CubeSats: A statistical look," *Journal of Small Satellites*, vol. 2, no. 2, pp. 213–233, 2013.

[35] "Small satellites: A revolution in space science," Keck Institute for Space Studies California Institute of Technology, Tech. Rep., 2014.

[36] A. Kestil, T. Tikka, , P. Peitso, J. Rantanen, A. Näsilä, K. Nordling, H. Saari, R. Vainio, P. Janhunen, J. Praks, and M. Hallikainen, "Aalto-1 nanosatellite — technical description and mission objectives," *Geosci. Instrum. Method. Data Syst.*, vol. 2, pp. 121–130, 2013.

[37] D. Rankin, D. D. Kekez, R. E. Zee, F. M. Pranajaya, D. G. Foisy, and A. M. Beattie, "The CanX-2 nanosatellite: Expanding the science abilities of nanosatellites," *Acta Astronaut.*, vol. 57, pp. 167–174, 2005.

[38] A. Scholz, W. Ley, B. Dachwald, J. Miau, and J. Juang, "Flight results of the COMPASS-1 picosatellite mission," *Acta Astronaut.*, vol. 67, pp. 1289–1298, 2010.

[39] J. Dickinson, C. DeForest, and T. Howard, "The CubeSat heliospheric imaging experiment (CHIME)," in *IEEE Aerospace Conference*, 2011.

[40] J. A. Larsen and K. Vinther, "Inexpensive CubeSat attitude estimation using COTS components and Unscented Kalman Filtering," in *5th International Conference on Recent Advances in Space Technologies*, 2011.

[41] C. R. McBryde and E. G. Lightsey, "A star tracker design for CubeSats," in *IEEE Aerospace Conference*, 2012.

[42] J. C. Springmann, A. J. Sloboda, A. T. Klesh, M. W. Bennett, and J. W. Cutler, "The attitude determination system of the RAX satellite," *Acta Astronaut.*, vol. 75, pp. 120–135, 2012.

[43] J. C. Springmann and J. W. Cutler, "Flight results of a low-cost attitude determination system," *Acta Astronaut.*, vol. 99, pp. 201–214, 2014.

[44] N. C. Deschamps, C. C. Grant, D. G.Foisy, R. E. Zee, A. F. Moffat, and W. W. Weiss, "The BRITE space telescope: Using a nanosatellite constellation to measure stellar variability in the most luminous stars," *Acta Astronaut.*, vol. 65, pp. 643–650, 2009.

[45] O. Koudelka, G.Egger, B. Josseck, N. Deschamp, C. C. Grant, D.Foisy, R. Zee, W.Weiss, R. Kuschnig, A. Scholtz, and W.Keim, "TUGSAT-1/BRITE-Austria — the first Austrian nanosatellite," *Acta Astronaut.*, vol. 64, pp. 1144–1149, 2009.

[46] D. Martinez, J. Quero, J. García, L. León, P. Castro, and C. Nieto, "Attitude determination module for CubeSat," in *IEEE International Conference on Industrial Technology*, 2015.

[47] A. Slavinskis, M. Pajusalu, H. Kuuste, E. Ilbis, Tõnis Eenmäe, I. Sünter, K. Laizāns, H. Ehrpais, P. Liias, E. Kulu, J. Viru, J. Kalde, U. Kvell, J. Kütt, K. Zalite, K. Kahn, S. Lätt, J. Envall, P. Toivanen, J. Polkko, P. Janhunen, R. Rosta, T. Kalvas, R. Vendt, V. Allik, and M. Noorma, "ESTCube-1 in-orbit experience and lessons learned," *IEEE Aerosp. Electron. Syst. Mag.*, vol. 30, no. 8, pp. 12–22, 2015.

[48] O. Khurshid, T. Tikka, J. Praks, and M. Hallikainen, "Accommodating the plasma brake experiment on-board the Aalto-1 satellite," *Proc. Estonian Acad. Sci.*, vol. 63(2S), pp. 258–266, 2014.

[49] *CubeSat Design Specification Rev. 13*, California Polytechnic State University Std., 2014.

[50] "Utilizing the potential of NANOSATellites for the implementation of European Space Policy and space innovation," Tartu Observatory, Database developed within an FP7 project, 2015. [Online]. Available: http://www.nanosats.eu/

[51] E. Kulu, A. Slavinskis, T. Eenmäe, E. Eilonen, L. Kimmel, and M. Noorma, "ESTCube-1 nanosatellite for electric solar wind sail demonstration in low earth orbit," in *64th International Astronautical Congress*, 2013.

[52] J. R. Wertz, Ed., *Spacecraft Attitude Determination and Control.* Kluwer Academic Publishers, 1978, ISBN: 978-9027712042.

[53] K. F. Jensen and K. Vinther, "Attitude determination and control system for AAUSAT3," Master's thesis, Aalborg University, 2010.

[54] R. A. Serway and J. W. Jewett, *Physics for Scientists and Engineers with Modern Physics*, 9th ed. Brooks Cole, 2013.

[55] D. Vallado and W. D. McClain, *Fundamentals of Astrodynamics and Applications.* Springer Science & Business Media, 2001.

[56] A. H. de Ruiter, C. Damaren, and J. R. Forbes, *Spacecraft Dynamics and Control: An Introduction*, 1st ed. Wiley, 2013.

[57] B. Wie, *Space Vehicle Dynamics and Control*, 2nd ed. The American Institute of Aeronautics and Astronautics, 2008.

[58] W. Ley, K. Wittmann, and W. Hallmann, *Handbook of Space Technology*. John Wiley & Sons, 2009.

[59] Metrology, *Evaluation of measurement data — Guide to the expression of uncertainty in measurement*, Joint Committee for Guides in Metrology Std., 2008.

[60] N. Olsen, L. Tøffner-Clausen, T. J. Sabaka, P. Brauer, J. M. G. Merayo, J. L. Jørgensen, J.-M. Léger, O. V. Nielsen, F. Primdahl, and T. Risbo, "Calibration of the Ørsted vector magnetometer," *Earth Planets Space*, vol. 55, pp. 11–18, 2003.

[61] M. Díaz-Michelena, "Small magnetic sensors for space applications," *Sensors*, vol. 9, pp. 2271–2288, 2009.

[62] C. Acar and A. Shkel, *MEMS Vibratory Gyroscopes: Structural Approaches to Improve Robustness*. Springer, 2009.

[63] F. R. Hoots and R. L. Roehrich, "Spacetrack report no. 3 — models for propagation of NORAD element sets," Peterson AFB: Office of Astrodynamics, Aerospace Defense Center, Tech. Rep., 1980.

[64] C. Hilton and J. Kuhlman, "Mathematical models for the space defense center," *Philco-Ford Publication No. U-3871*, pp. 17–28, 1966.

[65] M. Lane and F. Hoots, "Project space track report no. 2 — general perturbations theories derived from the 1965 lane drag theory," Aerospace Defense Command, Peterson AFB, CO, Tech. Rep., 1979.

[66] R. Hujsak, "A restricted four body solution for resonating satellites with an oblate Earth," *AIAA*, no. 79-136, 1979.

[67] F. Hoots, "A short, efficient analytical satellite theory," *J. Guid. Control. Dynam.*, vol. 5, no. 2, pp. 194–199, 1982.

[68] W. Dong and Z. Chang-yin, "An accuracy analysis of the SGP4/SDP4 model," *Chin. Astron. Astrophy.*, vol. 34, pp. 69–76, 2010.

[69] N. A. O. (US), Ed., *The Astronomical Almanac for the Year 2014*. Government Printing Office, 2013.

[70] R. T. Merrill, *The Magnetic Field of the Earth: Paleomagnetism, the Core, and the Deep Mantle*, M. W. McElhinny and P. L. McFadden, Eds. Academic Press, 1998, vol. 63.

[71] C. C. Finlay, N. Olsen, and L. Tøffner-Clausen, "DTU candidate field models for IGRF-12 and the CHAOS-5 geomagnetic field model," *Earth Planets Space*, vol. 67, no. 114, 2015.

[72] E. Thebault, C. C. Finlay, C. D. Beggan, P. Alken, J. Aubert, O. Barrois, F. Bertrand, T. Bondar, A. Boness, L. Brocco, E. Canet, A. Chambodut, A. Chulliat, P. Coisson, F. Civet, A. Du, A. Fournier, I. Fratter, N. Gillet, B. Hamilton, M. Hamoudi, G. Hulot, T. Jager, M. Korte, W. Kuang, X. Lalanne, B. Langlais, J.-M. Leger, V. Lesur, F. J. Lowes, S. Macmillan, M. Mandea, C. Manoj, S. Maus, N. Olsen, V. Petrov, V. Ridley, M. Rother, T. J. Sabaka, D. Saturnino, R. Schachtschneider, O. Sirol, A. Tangborn, A. Thomson, L. Toffner-Clausen, P. Vigneron, I. Wardinski, and T. Zvereva, "International Geomagnetic Reference Field: the 12th generation," *Earth Planets Space*, vol. 67, no. 79, 2015.

[73] A. Chulliat, S. Macmillan, P. Alken, C. Beggan, M. Nair, B. Hamilton, A. Woods, V. Ridley, S. Maus, and A. Thomson, "The US/UK world magnetic model for 2015–2020," National Geophysical Data Center, Tech. Rep., 2015.

[74] G. Haines and L. Newitt, "The Canadian Geomagnetic Reference Field," *Journal of Geomagnetism and Geoelectricity*, vol. 49, pp. 317–336, 1997.

[75] C. C. Finlay, S. Maus, C. D. Beggan, T. N. Bondar, A. Chambodut, T. A. Chernova, A. Chulliat, V. P. Golovkov, B. Hamilton, M. Hamoudi, R. Holme, G. Hulot, W. Kuang, B. Langlais, V. Lesur, F. J. Lowes, H. Lühr, S. Macmillan, M. Mandea, S. McLean, C. Manoj, M. Menvielle, I. Michaelis, N. Olsen, J. Rauberg, M. Rother, T. J. Sabaka, A. Tangborn, L. Tøffner-Clausen, E. Thébault, A. W. P. Thomson, I. W. Z. Wei, and T. I. Zvereva, "International Geomagnetic Reference Field: the eleventh generation," *Geophys. J. Int.*, vol. 183, no. 3, pp. 1216–1230, 2010.

[76] T. Bak, "Spacecraft attitude determination — a magnetometer approach," Ph.D. dissertation, Aalborg University, 1999.

[77] S. Maus, C. Manoj, J. Rauberg, I. Michaelis, and H. Lühr, "NOAA/NGDC candidate models for the 11th generation International

Geomagnetic Reference Field and the concurrent release of the 6th generation Pomme magnetic model," *Earth Planets Space*, vol. 62, pp. 729–735, 2010.

[78] O. Montenbruck and T. Pfleger, *Astronomy on the Personal Computer*, 2nd ed. Springer-Verlag, 1994, ISBN: 978-3-540-67221-0.

[79] H. D. Black, "A passive system for determining the attitude of a satellite," *AIAA Journal*, vol. 2, no. 7, pp. 1350–1351, 1964.

[80] M. D. Shuster and S. D. Oh, "Three-axis attitude determination from vector observations," *J. Guid. Control. Dynam.*, vol. 4, no. 1, pp. 70–77, 1981.

[81] P. B. Davenport, "A vector approach to the algebra of rotations with applications," NASA Goddard Space Flight Center, Tech. Rep., 1968.

[82] M. D. Shuster, "Approximate algorithms for fast optimal attitude computation," in *AIAA Guidance and Control Conference*, 1978.

[83] ——, "Algorithms for determining optimal attitude solutions," Goddard Space Flight Center, Tech. Rep., 1978.

[84] ——, "A survey of attitude representations," *J. Astronaut. Sci.*, vol. 41, no. 4, pp. 439–517, 1993.

[85] R. E. Kalman, "A new approach to linear filtering and prediction problems," *J. Basic. Eng.*, vol. 89 (D), pp. 35–45, 1960.

[86] G. Wahba, "A least squares estimate of spacecraft attitude," *SIAM Review*, vol. 8, no. 3, pp. 384–386, 1966.

[87] K. Vinther, K. F. Jensen, J. A. Larsen, and R. Wiśniewski, "Inexpensive CubeSat attitude estimation using quaternions and unscented Kalman filtering," *Online journal Automatic Control in Aerospace*, 2011.

[88] S. Haykin, Ed., *Kalman filtering and neural networks*. John Wiley & Sons, Inc., 2001.

[89] Autonomous Star Sensor ASTRO 15 Data Sheet. Jena-Optronik.

[90] Fine Sun Sensor Data Sheet. Jena-Optronik.

[91] STD 16 Earth Sensor Data Sheet. Sodern.

[92] GG1320AN Digital Laser Gyro Data Sheet. Honeywell.

[93] Honeywell HMC5883L product specification.

[94] Invensense ITG-3200 product specification.

[95] MAX1226/MAX1228/MAX1230 product specification.

[96] Hamamatsu S3931 product specification.

[97] H. Kuuste, T. Eenmäe, V. Allik, A. Agu, R. Vendt, I. Ansko, K. Laizāns, I. Sünter, S. Lätt, and M. Noorma, "Imaging system for nanosatellite proximity operations," *Proc. Estonian Acad. Sci.*, vol. 63(2S), pp. 250– 257, 2014.

[98] A. Slavinskis, U. Kvell, E. Kulu, T. Scheffler, S. Lätt, and M. Noorma, "Magnetic attitude control algorithms for ESTCube-1," in *63rd International Astronautical Congress*, 2012.

Acknowledgements

Curriculum Vitae

Name:	Andris Slavinskis
Address:	Observatooriumi 1, Tõravere, Tartu county, 61602, Estonia
Date of birth:	02.02.1988
Phone:	+37258284333
E-mail:	andris.slavinskis@estcube.eu

EDUCATION

2011 – *present*:	University of Tartu, Institute of Physics,
	PhD thesis topic: ESTCube-1 attitude determination
2009 – 2011:	Ventspils University College,
	Master study programme of Science in Computer Science
2010:	Lund University, exchange semester
2006 – 2009:	Ventspils University College,
	Bachelor study programme in Computer Science

EXPERIENCE

2012.01 – *present*:	junior researcher, Tartu Observatory, Space Technology Department
2013.09 – *present*:	guest lecturer, University of Tartu, Space Technology
2015.06 – *present*:	researcher, Robotiem Ltd.
2014.08 – 2015.05:	guest researcher, Finnish Meteorological Institute, Earth Observation Division
2011.02 – 2011.04:	trainee, Paul Scherrer Institute, Target Facilities and Activated Materials Group
2008.10 – 2011.01:	specialist, Engineering Research Institute
	"Ventspils International Radio Astronomy Centre" of Ventspils University College

RESEARCH

Journal articles

A. Slavinskis et al., ESTCube-1 In-Orbit Experience and Lessons Learned, *IEEE Aerosp. Electron. Syst. Mag.* **30**(8) (2015) 12–22.

A. Slavinskis et al., Flight Results of ESTCube-1 Attitude Determination System, *J. Aerospace Eng.*, DOI: 10.1061/(ASCE)AS.1943-5525.0000504 (2015) 04015014.

A. Slavinskis et al., Attitude determination and control for centrifugal tether deployment on the ESTCube-1 nanosatellite, *Proc. Estonian Acad. Sci.* **63**(2S) (2014) 242–249.

S. Lätt, **A. Slavinskis** et al., ESTCube-1 nanosatellite for electric solar wind sail in-orbit technology demonstration, *Proc. Estonian Acad. Sci.* **63**(2S) (2014) 200–209.

A. Slavinskis et al., High spin rate magnetic controller for nanosatellites, *Acta Astronaut.* **95** (2014) 218-226.

Conference proceedings

A. Slavinskis et al., ESTCube-1 student satellite in-orbit experience and lessons learned, *10th IAA Symposium on Small Satellites for Earth Observation* (2015).

E. Kulu, **A. Slavinskis** et al., ESTCube-1 nanosatellite for electric solar wind sail demonstration in low Earth orbit, *Proc. of 64th International Astronautical Congress* **5** (2013) 3898–3902.

M. Noorma, **A. Slavinskis** et al., Estonian Student Satellite Program, *Proc. of 64th International Astronautical Congress* (2013).

A. Slavinskis et al., Magnetic Attitude Control Algorithms for ESTCube-1, *Proc. of 63rd International Astronautical Congress* **6** (2012) 4475–4480.

Posters

A. Slavinskis et al., Nanosatellite technology for Solar System exploration, *Formation and evolution of planetary systems and habitable planets*, Molėtai, Lithuania, 2015.

A. Slavinskis et al., ESTCube-1 attitude determination: in-flight experience, *Small Satellites and Services Symposium*, Majorca, Spain, 2014.

R. Valner, **A. Slavinskis** et al., Low-Power Custom-Built Sun Sensors For Nanosatellite, *Physics Days*, Espoo, Finland, 2013.

E. Kulu, **A. Slavinskis**, U. Kvell, Attitude Determination and Control System for ESTCube-1, *Estonian Physics Days*, Tartu, 2012.

Other conferences and seminars

Invited talk: ESTCube-1 in-orbit experience and lessons learned. *Seminar*, University of Latvia, Riga, Latvia, 23.10.2015.

ESTCube-1 attitude determination. *PhD thesis seminar*, University of Tartu, Institute of Physics, Tartu, Estonia, 12.10.2015.

ESTCube-1 bus: in-orbit experience and lessons learned. *Seminar*, Finnish Meteorological Institute, Helsinki, Finland, 28.11.2014.

Invited talk: ESTCube-1 in-orbit experience and lessons learned. *Seminar*, Royal Institute of Technology, Stockholm, Sweden, 06.11.2014.

ESTCube-1 attitude determination and camera flight results. *Tartu Conference on Space Science and Technology*, Tartu, Estonia, 22.09.2014.

ESTCube-1 status report. European Space Research and Technology Centre, Noordwijk, Netherlands, 15.07.2014.

Exhibition stand. *International Conference and Exhibition on Space Technologies*, Riga, Latvia, 05-06.06.2014.

ESTCube-1 camera design and characterization. *Small Satellites and Services Symposium*, Majorca, Spain, 28.05.2014.

ESTCube-1 progress report. *Estonian Physics Days*, Tartu, Estonia, 21.03.2014.

ESTCube-1 nanosatellite: Electric solar wind sail demonstration. *University of Latvia Annual Conference*, Riga, Latvia, 05.02.2014.

Attitude determination and control of ESTCube-1. *Baltic Applied Astroinformatics and Space Data Processing*, Ventspils, Latvia, 16.05.2013.

Solar Wind Electric Sail Testing CubeSat: mission concept. *Baltic Applied Astroinformatics and Space Data Processing*, Ventspils, Latvia, 16.05.2013.

Spin-up of ESTCube-1 for E-sail experiment. *Aalto CubeSat course*, Espoo, Finland, 09.05.2012.

Theses

A. Slavinskis, MSc, 2011, (sup) N. Jēkabsons, S. Dementjevs, R. Milenković, Optimization of SINQ (Swiss Spallation Neutron Source) target cooling; development of measurement system for thermohydraulic and structural-mechanical experiments (in Latvian), Ventspils University College.

A. Slavinskis, BSc, 2009, (sup) J. Hofmanis, Development of Prototype for Geological Technology Data Mathematical Systematization (in Latvian), Ventspils University College.

PROJECTS

Receiving, validation and bootloading system of small satellite software as an enabler for safe and reliable satellite development and utilisation. Latvian Electronic and Optical Equipment Competence Centre in Production Sector, 2015.

Technology demonstration for space debris mitigation and electric propulsion on ESTCube-1 student satellite. European Space Agency Plan for European Cooperating States, 2013.

OUTREACH

A. Slavinskis, Estonian satellite has finished the mission (in Latvian), *Ilustrētā Zinātne* **114** (2015) 24–25.

A. Slavinskis, K. Kalniņa, Do we want to return to a country with discrimination? (in Latvian), *Ir*, 21.04.2015.

An interview about space technologies for development of agriculture of Latvia. (in Latvian), *Radio Latvia 1*, 23.03.2015.

A. Slavinskis, About cooperation of Latvia with the European Space Agency (in Latvian), *Zvaigžņotā*

Debess **227** (2015) 65–67.

A. Slavinskis, Is the government sabotaging the country by not cooperating with the European Space Agency? (in Latvian), *Ir*, 05.01.2015.

A. Slavinskis, K. Kalniņa, The first Tartu Conference on Space Science and Technology has taken place (in Latvian), *StarSpace*, 30.09.2014.

An interview about the career in space technologies (in Latvian), *StarSpace StarParty #12*, 06.09.2014.

A. Slavinskis, From the first man-made fire to sailing in the space (in Latvian), *Zvaigžņotā Debess* **224** (2014) 23–27.

A. Slavinskis, Estonian students at the frontier of scientific and technological development, *TEDxYouth@Tallinn*, 16.11.2013.

An interview about the ESTCube-1 project, *miks.ee*, 27.01.2014.

COURSES

2015.08: Formation and evolution of planetary systems and habitable planets, Molėtai, Lithuania
2013.08: International Summer Space School, Samara State Aerospace University, Russia
2012.05: Aalto CubeSat course, Aalto University, Finland

LANGUAGE

Latvian: native proficiency
English: full professional proficiency
Estonian: elementary proficiency

SCHOLARSHIPS

2011.12 – 2015.11: Scholarship for PhD studies, ESF DoRa programme activity 4:
Doctoral studies of talented international students in Estonian universities
2014.01 – 2014.05 Scholarship for visiting Finnish Meteorological Institute, Erasmus+ traineeship grant
2014.08 – 2015.01: Scholarship for visiting Finnish Meteorological Institute,
ESF DoRa programme activity 6: Development of international cooperation
networks by supporting the mobility of Estonian doctoral students
2014.10: Scholarship for work on ESTCube-1, Tartu Observatory: Charles Villmann fellowship
2012.10: Scholarship for attending International Astronautical Congress,
Kristjan Jaak grant for foreign visits
2009.09 – 2011.06 Scholarship for master studies, ESF: Support for implementation of computer science
curriculum in Ventspils University College, Information Technology Faculty
2010.01 – 2010.05 Scholarship for exchange studies, Erasmus study scholarship
2006 - 2009: Scholarship for bachelor studies, State scholarship

OTHER ACTIVITIES

2015.05 – *present*: ESTCube Programme leader
2014.01 – 2014.06: ESTCube Programme international student coordinator
2013.03: Aalto-2 preliminary design review panellist
2012.03 – 2014.03: ESTCube-1 attitude determination and control system leader
2012.03: ESTELLE feasibility study
2011.01: establisher of a folk dancing group *Strautuguns*
2010.09 – 2011.06: member of the Constitutional assembly of Ventspils University College

Elulookirjeldus

Nimi:	Andris Slavinskis
Aadress:	Observatooriumi 1, Tõravere, Tartumaa, 61602, Eesti
Sünniaeg:	02.02.1988
Telefoninumber:	+37258284333
E-posti aadress:	andris.slavinskis@estcube.eu

HARIDUS

2011 – ...:	Tartu Ülikooli Füüsika Instituut, PhD füüsikas
2009 – 2011:	Ventspilsi Ülikooli Kolledž, M. Sc. arvutiteaduses
2010:	Lundi Ülikool, välisõpe
2006 – 2009:	Ventspilsi Ülikooli Kolledž, B. Sc. arvutiteaduses

TÖÖKOHAD

2012.01 – ...:	noorem teadur, Tartu Observatoorium, Kosmosetehnoloogia osakond
2013.09 – ...:	külalislektor, Tartu Ülikool, Kosmosetehnoloogia
2015.06 – ...:	teadur, Robotiem OÜ
2014.08 – 2015.05:	külalisteadur, Soome Meteoroloogia Instituut
2011.02 – 2011.04:	praktikant, Paul Scherreri Instituut
2008.10 – 2011.01:	spetsialist, Inseneriteaduse Instituut, Ventspilsi Ülikooli Kolledž

TEADUSTÖÖ

Teaduslikud artiklid

A. Slavinskis et al., ESTCube-1 In-Orbit Experience and Lessons Learned, *IEEE Aerosp. Electron. Syst. Mag.* **30**(8) (2015) 12–22.

A. Slavinskis et al., Flight Results of ESTCube-1 Attitude Determination System, *J. Aerospace Eng.*, DOI: 10.1061/(ASCE)AS.1943-5525.0000504 (2015) 04015014.

A. Slavinskis et al., Attitude determination and control for centrifugal tether deployment on the ESTCube-1 nanosatellite, *Proc. Estonian Acad. Sci.* **63**(2S) (2014) 242–249.

S. Lätt, **A. Slavinskis** et al., ESTCube-1 nanosatellite for electric solar wind sail in-orbit technology demonstration, *Proc. Estonian Acad. Sci.* **63**(2S) (2014) 200–209.

A. Slavinskis et al., High spin rate magnetic controller for nanosatellites, *Acta Astronaut.* **95** (2014) 218-226.

Konverentside artiklid

A. Slavinskis et al., ESTCube-1 student satellite in-orbit experience and lessons learned, *10th IAA Symposium on Small Satellites for Earth Observation* (2015).

E. Kulu, **A. Slavinskis** et al., ESTCube-1 nanosatellite for electric solar wind sail demonstration in low Earth orbit, *Proc. of 64th International Astronautical Congress* **5** (2013) 3898–3902.

M. Noorma, **A. Slavinskis** et al., Estonian Student Satellite Program, *Proc. of 64th International Astronautical Congress* (2013).

A. Slavinskis et al., Magnetic Attitude Control Algorithms for ESTCube-1, *Proc. of 63rd International Astronautical Congress* **6** (2012) 4475–4480.

Postrid

A. Slavinskis et al., Nanosatellite technology for Solar System exploration, *Formation and evolution of planetary systems and habitable planets*, Molėtai, Leedu, 2015.

A. Slavinskis et al., ESTCube-1 attitude determination: in-flight experience, *Small Satellites and Services Symposium*, Mallorca, Hispaania, 2014.

R. Valner, **A. Slavinskis** et al., Low-Power Custom-Built Sun Sensors For Nanosatellite, *Physics Days*, Espoo, Soome, 2013.

E. Kulu, **A. Slavinskis**, U. Kvell, Attitude Determination and Control System for ESTCube-1, *Eesti füüsikapäevad*, Tartu, 2012.

Lõputööd

A. Slavinskis, MSc, 2011, (sup) N. Jēkabsons, S. Dementjevs, R. Milenković, SINQ (Šveices infrastruktūra neitronu atskaldīšanai) mērķa dzesēšanas optimizācija; mērījumu veikšanas sistēmas izstrāde termohidrauliskiem un materiālu pretestības eksperimentiem (läti keeles), Ventspilsi Ülikooli Kolledž.

A. Slavinskis, BSc, 2009, (sup) J. Hofmanis, Ģeoloģiskās izpētes datu matemātiskās sistematizācijas tehnoloģijas prototipa izstrāde (läti keeles), Ventspilsi Ülikooli Kolledž.

KOOLITUSED

2015.08:	Planeedisüsteemide ja elamiskõlblikku planeetide tekkimine ja areng, Molėtai, Leedu
2013.08:	Rahvusvaheline Kosmose Suvekool, Samara Riiklik Ülikool, Venemaa
2012.05:	Aalto CubeSat kursus, Aalto Ülikool, Soome

KEELED

Läti:	emakeel
Inglise:	kõrgtase
Eesti:	algtase

STIPENDIUMID

2011.12 – 2015.11:	Stipendium õpingute doktoriõppes jaoks, ESF DoRa programmi tegevus 4: Välisüliõpilaste kaasamine doktoriõppesse
2014.01 – 2014.05	Erasmus+ programmi stipendium Soome Meteoroloogia Instituudi külastamisekss
2014.08 – 2015.01:	Stipendium Soome Meteoroloogia Instituudi külastamiseks, ESF DoRa programmi tegevus 8: Noorteadlase osalemine rahvusvahelises teadmiste ringluses
2014.10:	Ch. Villmanni nimeline stipendium (kosmosetehnoloogia) Tartu Observatooriumilt töö ESTCube-1 projektis eest
2012.10:	Kristjan Jaagu välissõidu stipendium konverentsil International Astronautical Congress osalemiseks
2009.09 – 2011.06	Ventspilsi Ülikooli Kolledži stipendium
2010.01 – 2010.05	Erasmus programmi stipendium õpingute Lundi Ülikoolis jaoks
2006 - 2009:	Ventspilsi Ülikooli Kolledži stipendium

DISSERTATIONES PHYSICAE
UNIVERSITATIS TARTUENSIS

1. **Andrus Ausmees.** XUV-induced electron emission and electron-phonon interaction in alkali halides. Tartu, 1991.
2. **Heiki Sõnajalg.** Shaping and recalling of light pulses by optical elements based on spectral hole burning. Tartu, 1991.
3. **Sergei Savihhin.** Ultrafast dynamics of F-centers and bound excitons from picosecond spectroscopy data. Tartu, 1991.
4. **Ergo Nõmmiste.** Leelishalogeniidide röntgenelektronemissioon kiiritamisel footonitega energiaga 70–140 eV. Tartu, 1991.
5. **Margus Rätsep.** Spectral gratings and their relaxation in some low-temperature impurity-doped glasses and crystals. Tartu, 1991.
6. **Tõnu Pullerits.** Primary energy transfer in photosynthesis. Model calculations. Tartu, 1991.
7. **Olev Saks.** Attoampri diapasoonis voolude mõõtmise füüsikalised alused. Tartu, 1991.
8. **Andres Virro.** AlGaAsSb/GaSb heterostructure injection lasers. Tartu, 1991.
9. **Hans Korge.** Investigation of negative point discharge in pure nitrogen at atmospheric pressure. Tartu, 1992.
10. **Jüri Maksimov.** Nonlinear generation of laser VUV radiation for high-resolution spectroscopy. Tartu, 1992.
11. **Mark Aizengendler.** Photostimulated transformation of aggregate defects and spectral hole burning in a neutron-irradiated sapphire. Tartu, 1992.
12. **Hele Siimon.** Atomic layer molecular beam epitaxy of A^2B^6 compounds described on the basis of kinetic equations model. Tartu, 1992.
13. **Tõnu Reinot.** The kinetics of polariton luminescence, energy transfer and relaxation in anthracene. Tartu, 1992.
14. **Toomas Rõõm.** Paramagnetic H^{2-} and F^+ centers in CaO crystals: spectra, relaxation and recombination luminescence. Tallinn, 1993.
15. **Erko Jalviste.** Laser spectroscopy of some jet-cooled organic molecules. Tartu, 1993.
16. **Alvo Aabloo.** Studies of crystalline celluloses using potential energy calculations. Tartu, 1994.
17. **Peeter Paris.** Initiation of corona pulses. Tartu, 1994.
18. **Павел Рубин.** Локальные дефектные состояния в CuO_2 плоскостях высокотемпературных сверхпроводников. Тарту, 1994.
19. **Olavi Ollikainen.** Applications of persistent spectral hole burning in ultra-fast optical neural networks, time-resolved spectroscopy and holographic interferometry. Tartu, 1996.
20. **Ülo Mets.** Methodological aspects of fluorescence correlation spectroscopy. Tartu, 1996.
21. **Mikhail Danilkin.** Interaction of intrinsic and impurity defects in CaS:Eu luminophors. Tartu, 1997.

22. **Ирина Кудрявцева.** Создание и стабилизация дефектов в кристаллах KBr, KCl, RbCl при облучении ВУФ-радиацией. Тарту, 1997.
23. **Andres Osvet.** Photochromic properties of radiation-induced defects in diamond. Tartu, 1998.
24. **Jüri Örd.** Classical and quantum aspects of geodesic multiplication. Tartu, 1998.
25. **Priit Sarv.** High resolution solid-state NMR studies of zeolites. Tartu, 1998.
26. **Сергей Долгов.** Электронные возбуждения и дефектообразование в некоторых оксидах металлов. Тарту, 1998.
27. **Kaupo Kukli.** Atomic layer deposition of artificially structured dielectric materials. Tartu, 1999.
28. **Ivo Heinmaa.** Nuclear resonance studies of local structure in $RBa_2Cu_3O_{6+x}$ compounds. Tartu, 1999.
29. **Aleksander Shelkan.** Hole states in CuO_2 planes of high temperature superconducting materials. Tartu, 1999.
30. **Dmitri Nevedrov.** Nonlinear effects in quantum lattices. Tartu, 1999.
31. **Rein Ruus.** Collapse of 3d (4f) orbitals in 2p (3d) excited configurations and its effect on the x-ray and electron spectra. Tartu, 1999.
32. **Valter Zazubovich.** Local relaxation in incommensurate and glassy solids studied by Spectral Hole Burning. Tartu, 1999.
33. **Indrek Reimand.** Picosecond dynamics of optical excitations in GaAs and other excitonic systems. Tartu, 2000.
34. **Vladimir Babin.** Spectroscopy of exciton states in some halide macro- and nanocrystals. Tartu, 2001.
35. **Toomas Plank.** Positive corona at combined DC and AC voltage. Tartu, 2001.
36. **Kristjan Leiger.** Pressure-induced effects in inhomogeneous spectra of doped solids. Tartu, 2002.
37. **Helle Kaasik.** Nonperturbative theory of multiphonon vibrational relaxation and nonradiative transitions. Tartu, 2002.
38. **Tõnu Laas.** Propagation of waves in curved spacetimes. Tartu, 2002.
39. **Rünno Lõhmus.** Application of novel hybrid methods in SPM studies of nanostructural materials. Tartu, 2002.
40. **Kaido Reivelt.** Optical implementation of propagation-invariant pulsed free-space wave fields. Tartu, 2003.
41. **Heiki Kasemägi.** The effect of nanoparticle additives on lithium-ion mobility in a polymer electrolyte. Tartu, 2003.
42. **Villu Repän.** Low current mode of negative corona. Tartu, 2004.
43. **Алексей Котлов.** Оксианионные диэлектрические кристаллы: зонная структура и электронные возбуждения. Tartu, 2004.
44. **Jaak Talts.** Continuous non-invasive blood pressure measurement: comparative and methodological studies of the differential servo-oscillometric method. Tartu, 2004.
45. **Margus Saal.** Studies of pre-big bang and braneworld cosmology. Tartu, 2004.

46. **Eduard Gerškevitš.** Dose to bone marrow and leukaemia risk in external beam radiotherapy of prostate cancer. Tartu, 2005.

47. **Sergey Shchemelyov.** Sum-frequency generation and multiphoton ionization in xenon under excitation by conical laser beams. Tartu, 2006.

48. **Valter Kiisk.** Optical investigation of metal-oxide thin films. Tartu, 2006.

49. **Jaan Aarik.** Atomic layer deposition of titanium, zirconium and hafnium dioxides: growth mechanisms and properties of thin films. Tartu, 2007.

50. **Astrid Rekker.** Colored-noise-controlled anomalous transport and phase transitions in complex systems. Tartu, 2007.

51. **Andres Punning.** Electromechanical characterization of ionic polymer-metal composite sensing actuators. Tartu, 2007.

52. **Indrek Jõgi.** Conduction mechanisms in thin atomic layer deposited films containing TiO_2. Tartu, 2007.

53. **Aleksei Krasnikov.** Luminescence and defects creation processes in lead tungstate crystals. Tartu, 2007.

54. **Küllike Rägo.** Superconducting properties of MgB_2 in a scenario with intra- and interband pairing channels. Tartu, 2008.

55. **Els Heinsalu.** Normal and anomalously slow diffusion under external fields. Tartu, 2008.

56. **Kuno Kooser.** Soft x-ray induced radiative and nonradiative core-hole decay processes in thin films and solids. Tartu, 2008.

57. **Vadim Boltrushko.** Theory of vibronic transitions with strong nonlinear vibronic interaction in solids. Tartu, 2008.

58. **Andi Hektor.** Neutrino Physics beyond the Standard Model. Tartu, 2008.

59. **Raavo Josepson.** Photoinduced field-assisted electron emission into gases. Tartu, 2008.

60. **Martti Pärs.** Study of spontaneous and photoinduced processes in molecular solids using high-resolution optical spectroscopy. Tartu, 2008.

61. **Kristjan Kannike.** Implications of neutrino masses. Tartu, 2008.

62. **Vigen Issahhanjan.** Hole and interstitial centres in radiation-resistant MgO single crystals. Tartu, 2008.

63. **Veera Krasnenko.** Computational modeling of fluorescent proteins. Tartu, 2008.

64. **Mait Müntel.** Detection of doubly charged higgs boson in the CMS detector. Tartu, 2008.

65. **Kalle Kepler.** Optimisation of patient doses and image quality in diagnostic radiology. Tartu, 2009.

66. **Jüri Raud.** Study of negative glow and positive column regions of capillary HF discharge. Tartu, 2009.

67. **Sven Lange.** Spectroscopic and phase-stabilisation properties of pure and rare-earth ions activated ZrO_2 and HfO_2. Tartu, 2010.

68. **Aarne Kasikov.** Optical characterization of inhomogeneous thin films. Tartu, 2010.

69. **Heli Valtna-Lukner.** Superluminally propagating localized optical pulses. Tartu, 2010.
70. **Artjom Vargunin.** Stochastic and deterministic features of ordering in the systems with a phase transition. Tartu, 2010.
71. **Hannes Liivat.** Probing new physics in e+e− annihilations into heavy particles via spin orientation effects. Tartu, 2010.
72. **Tanel Mullari.** On the second order relativistic deviation equation and its applications. Tartu, 2010.
73. **Aleksandr Lissovski.** Pulsed high-pressure discharge in argon: spectroscopic diagnostics, modeling and development. Tartu, 2010.
74. **Aile Tamm.** Atomic layer deposition of high-permittivity insulators from cyclopentadienyl-based precursors. Tartu, 2010.
75. **Janek Uin.** Electrical separation for generating standard aerosols in a wide particle size range. Tartu, 2011.
76. **Svetlana Ganina.** Hajusandmetega ülesanded kui üks võimalus füüsika-õppe efektiivsuse tõstmiseks. Tartu, 2011
77. **Joel Kuusk.** Measurement of top-of-canopy spectral reflectance of forests for developing vegetation radiative transfer models. Tartu, 2011.
78. **Raul Rammula**. Atomic layer deposition of HfO_2 – nucleation, growth and structure development of thin films. Tartu, 2011.
79. **Сергей Наконечный.** Исследование электронно-дырочных и интерстициал-вакансионных процессов в монокристаллах MgO и LiF методами термоактивационной спектроскопии. Тарту, 2011.
80. **Niina Voropajeva.** Elementary excitations near the boundary of a strongly correlated crystal. Tartu, 2011.
81. **Martin Timusk.** Development and characterization of hybrid electro-optical materials. Tartu, 2012, 106 p.
82. **Merle Lust.** Assessment of dose components to Estonian population. Tartu, 2012, 84 p.
83. **Karl Kruusamäe.** Deformation-dependent electrode impedance of ionic electromechanically active polymers. Tartu, 2012, 128 p.
84. **Liis Rebane.** Measurement of the $W \to \tau\nu$ cross section and a search for a doubly charged Higgs boson decaying to τ-leptons with the CMS detector. Tartu, 2012, 156 p.
85. **Jevgeni Šablonin.** Processes of structural defect creation in pure and doped MgO and NaCl single crystals under condition of low or super high density of electronic excitations. Tartu, 2013, 145 p.
86. **Riho Vendt**. Combined method for establishment and dissemination of the international temperature scale. Tartu, 2013, 108 p.
87. **Peeter Piksarv.** Spatiotemporal characterization of diffractive and non-diffractive light pulses. Tartu, 2013, 156 p.
88. **Anna Šugai.** Creation of structural defects under superhigh-dense irradiation of wide-gap metal oxides. Tartu, 2013, 108 p.

89. **Ivar Kuusik.** Soft X-ray spectroscopy of insulators. Tartu, 2013, 113 p.
90. **Viktor Vabson**. Measurement uncertainty in Estonian Standard Laboratory for Mass. Tartu, 2013, 134 p.
91. **Kaupo Voormansik.** X-band synthetic aperture radar applications for environmental monitoring. Tartu, 2014, 117 p.
92. **Deivid Pugal.** hp-FEM model of IPMC deformation. Tartu, 2014, 143 p.
93. **Siim Pikker.** Modification in the emission and spectral shape of photostable fluorophores by nanometallic structures. Tartu, 2014, 98 p.
94. **Mihkel Pajusalu**. Localized Photosynthetic Excitons. Tartu, 2014, 183 p.
95. **Taavi Vaikjärv.** Consideration of non-adiabaticity of the Pseudo-Jahn-Teller effect: contribution of phonons. Tartu, 2014, 129 p.
96. **Martin Vilbaste.** Uncertainty sources and analysis methods in realizing SI units of air humidity in Estonia. Tartu, 2014, 111 p.
97. **Mihkel Rähn.** Experimental nanophotonics: single-photon sources- and nanofiber-related studies. Tartu, 2015, 107 p.
98. **Raul Laasner.** Excited state dynamics under high excitation densities in tungstates. Tartu, 2015, 125 p.